August 2020

Evaluation of One Piece in the Blood Coagulation Puzzle: Exploring an Activation Mechanism of Tissue Factor Through Self-association

Brittany S. Vanderhoof
University of Wisconsin-Milwaukee

EVALUATION OF ONE PIECE IN THE BLOOD COAGULATION PUZZLE: EXPLORING AN ACTIVATION MECHANISM OF TISSUE FACTOR THROUGH SELF-ASSOCIATION

by

Brittany Vanderhoof

A Thesis Submitted in

Partial Fulfillment of the

Requirements for the Degree of

Master of Science

In Biological Sciences

at

The University of Wisconsin-Milwaukee

August 2020

ABSTRACT

EVALUATION OF ONE PIECE IN THE BLOOD COAGULATION PUZZLE: EXPLORING AN ACTIVATION MECHANISM OF TISSUE FACTOR THROUGH SELF-ASSOCIATION

by

Brittany Vanderhoof

The University of Wisconsin-Milwaukee, 2020
Under the Supervision of Professor Julie Oliver, Ph.D

Tissue Factor (TF) is a transmembrane protein that is the physiologically relevant initiator of blood coagulation. The proteolytic reactions by which the complex of TF with activated coagulation factor VII (TF-FVIIa) activates factor X (FX) to FXa, ultimately leading to production of thrombin and fibrin clot formation has been established. The mechanism by which TF becomes activated from a non-coagulant state remains unclear. One of the competing hypotheses, the TF self-association hypothesis, proposes that oligomerization blocks the docking site for FXa thereby reducing the pro-coagulant activity. Another hypothesis, the allosteric disulfide bond hypothesis, proposes that the redox state causes a conformational change in TF that can affect FXa generation. Resting and stimulated lymphocyte derived cells were analyzed for oligomeric structure. We have shed light on the self-association hypothesis and based on results obtained; conclude that TF self-association may not be responsible for the transformation of TF into a procoagulant form.

DEDICATION

To my friends, especially Abby, for lifting my spirits during tough times. And of course, I dedicate this to my family. To my mother, who gave me the greatest gift of all, life. To my sisters, I despised you when we were young but have unconditional love for now. My brother-in-laws who make me laugh, my niece and nephews who keep me on my toes, and any children I might have; “hi kid(s)”. Last but not least I dedicate this to my two favorite men. Charlie, my significant other, who has loved, inspired, and supported me for a decade. Also to my father, who has taught me a vast amount of knowledge, from wrenching on automobiles to the universe. Dad, you have been there for me every step of the way throughout my entire life and I could not have accomplished what I have without you.

TABLE OF CONTENTS

LIST OF FIGURES

LIST OF TABLES

LIST OF ABBREVIATIONS

TF	Tissue factor
F.X(a)	Factor X(a)
F.VIIa	Factor VIIa
FRET	Förster resonance energy transfer
E_{app}	Apparent FRET efficiency
GLA	γ-carboxyglutamic acid
PDI	Protein disulfide isomerase
TFPI	Tissue factor pathway inhibitor
PS	phosphatidylserine
mTq	monomeric turquoise
SYFP2	Super yellow fluorescent protein 2
PMA	Phorbol myristate acetate
LPS	lipopolysaccharide
ROI	Region of interest

ACKNOWLEDGEMENTS

First and foremost, I would like to thank my advisor, Julie Oliver, for giving me the opportunity to take part in this research project. She has been a great mentor and her vision, guidance, and encouragement, has inspired me. I am very appreciative for what she has offered me and enjoyed working with her as she is kind, motivating, has challenged me, and has a wonderful sense of humor. I would like to thank my committee members, Heather Owen and Valerica Raicu; I could not have asked for a better committee. They have been kind, insightful, supplied me with necessary tools, and suggestions with enthusiasm; without them I would not have been able to complete this project. I also received an abundance of help from Doug Steeber and Chuck Wimpee, in fact I consider them my honorary committee members and I would like to thank them for all they have done to assist with this project. Thanks to the Oliver lab and Steeber lab members Cammy Truong, Samer Alanani, and especially Ryan Nelson who assisted with cell culture. Thanks to member of the Raicu group especially Mike Stoneman, Gabby Biener, and Dammar Badu for all the time spent helping with data analysis and FRET measurements. Thanks to Paul Park and Megan Gragg for providing plasmids with fluorophores needed for FRET experiments. Thanks to L-C Petersen for supplying cDNA of human TF. Lastly thanks to many un-named professors and graduate students in the department of biological sciences who have provided me with ideas and necessary tools and reagents for this research.

I: A tale of TF

Tissue Factor (TF) is a transmembrane protein that is the physiologically relevant initiator of coagulation. TF activity results in a well-characterized cascade of proteolytic reactions that lead to clotting; however, the mechanism by which TF is activated remains to be elucidated. TF is essential to normal development and life functions. Animals engineered to be genetically deficient in TF (TF knock-out animals) have an embryonic lethal phenotype and display severe hemostatic deficiencies. However, in a variety of pathological conditions such as acute or chronic inflammation, TF can be aberrantly expressed or activated, leading to thrombotic disease.

TF exists in dual states: cryptic TF is the non-coagulant state, whereas decrypted TF is the procoagulant version that results from an activation event. It is well known that the exposure of negatively charged phospholipids on the outer leaflet of the cell membrane is essential for TF procoagulant function; however, a mechanism independent of phospholipid rearrangement is also involved. Several proposals have described how TF might transform into a procoagulant protein, including alteration of the redox state, glycosylation, and the self-association of TF molecules. There are two main competing hypotheses describing how TF activation takes place. The first, the allosteric disulfide bond hypothesis, states that when the Cys186-Cys209 disulfide bond is reduced, a conformational change occurs that transforms TF into its procoagulant form. The second is the self-association hypothesis: TF molecules can form dimers within the membrane, and this keeps TF in a cryptic state by obstructing the docking site for factor X (F.X) at the interface of the homodimers. The inability of the substrate, F.X, to bind

to TF and form an initiation complex would absolutely block procoagulant activity. Therefore, we hypothesize that TF exists as oligomers on quiescent cells, and upon cellular activation, these oligomers dissociate and leave the protein fully active to initiate coagulation.

We have tested this hypothesis by genetically engineering plasmids to express a fluorescent protein fused to the C-terminus of TF. After creating mammalian expression plasmids, murine pre-B cells were transfected with linearized DNA that encoded for TF-fluorophore fusion proteins. Förster resonance energy transfer (FRET) experiments were conducted on transfected cells with and without activating agents. A separate set of experiments explored the effect of applying different concentrations of the TF ligand factor VIIa (F.VIIa). Finally, analysis was completed to assess the oligomeric structure and evaluate if the degree of oligomerization changed with activation or concentration of F.VIIa (Figure 1).

It is generally assumed reporter moieties have no effect on protein function. Our system is unique in that we have the ability to directly test whether that assumption is correct. We addressed the question of whether the addition of a fluorophore to the C-terminus of the TF molecule has an effect on its procoagulant activity. The original heterogenous populations of fluorophore-conjugated and unconjugated TF transfectants were subcloned to create a library of cell lines with similar levels of TF expressed on their surfaces. The procoagulant activity of lines with similar levels of fluorophore-conjugated and unconjugated TF expression was compared by assaying their ability to support activation of F.X to F.Xa in the presence of F.VIIa.

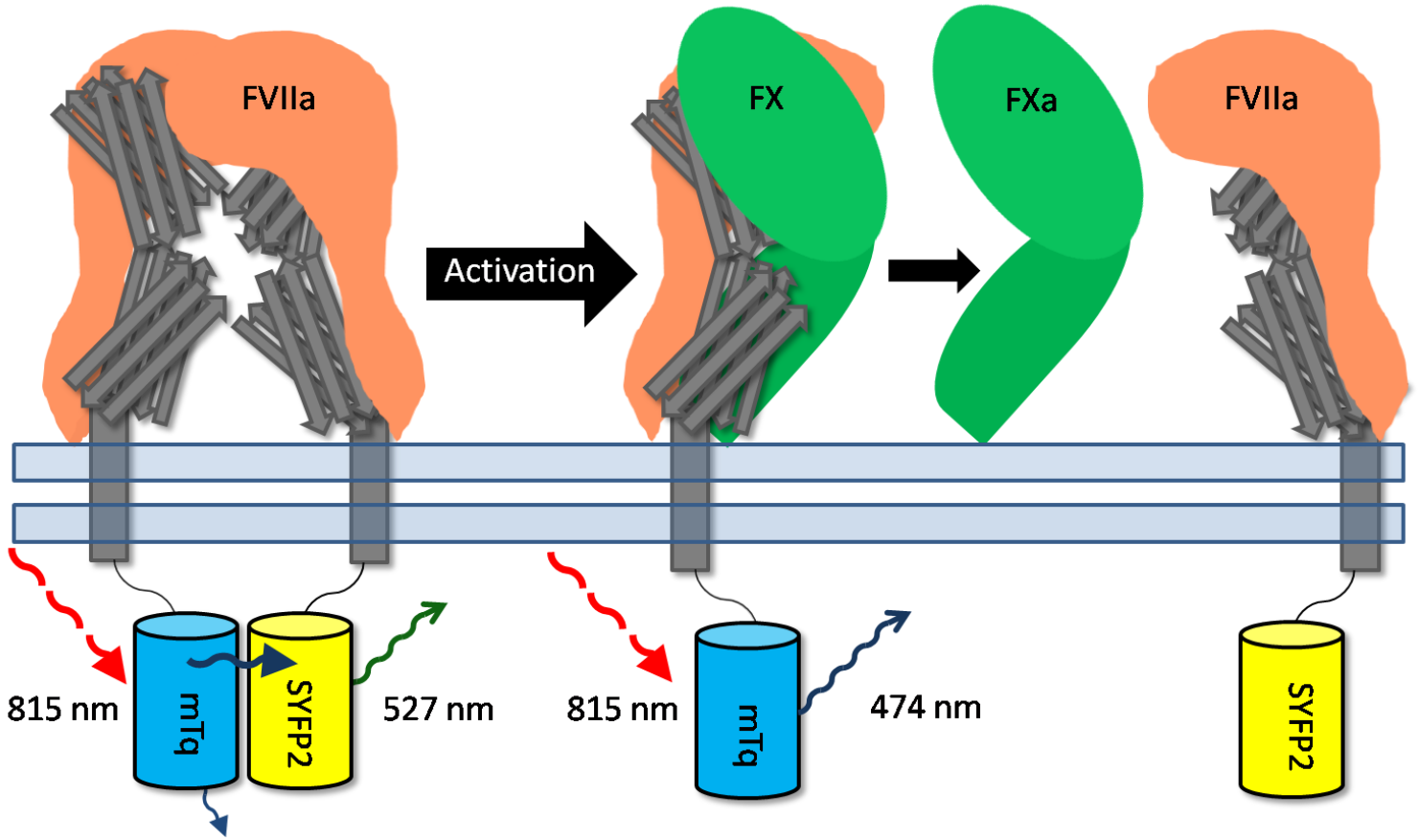

Figure 1: TF self-association hypothesis. TF fusion proteins tagged with donor (m-Turquoise, mTq) or acceptor (super yellow fluorescent protein 2, SYFP2) fluorophores. Excitation of the donor fluorophore is illustrated as it occurs during two-photon microscopy. When TF molecules are oligomerized they are able to bind F.VIIa, yet are in a cryptic state in which substrate F.X is hindered from binding at its docking site. When this occurs, energy will be transferred from the donor to the acceptor fluorophore and FRET signal will be observed as emission from the acceptor fluorophore. When the molecules are dissociated due to cell activation, energy from the donor will be lost as fluorescence and TF will be able to initiate coagulation by TF-F.VIIa cleavage of F.X into F.Xa. The TF-F.VIIa complex would be equally capable of activating F.X to F.Xa whether fused to mTq (as shown) or SYFP2 (not shown).

II: Lessons from the Literature

A. A Brief History

Coagulation has intrigued scientific minds for generations, with thoughts evolving into our current description of the coagulation cascade. It had been observed since 1834[1] that when blood came into contact with tissues, clotting was much faster both in vivo and in vitro than in the absence of exposure to tissue. Marowitz proposed a clotting theory in 1905, consisting of four different factors. These were thrombokinase or factor III (now known as TF), prothrombin (F.II), calcium (F.IV), and fibrinogen (F.I).[1,2,3] Starting In the 1930s tests were created to test blood clotting time, and thereafter many coagulation factors were discovered such as VII, V, and X because unique patients had deficiencies in clotting times.[1] Over time additional factors were discovered and in the 1960s the evolution of the cascade theory for initiating the intrinsic coagulation pathway was proposed independently by Macfarlane and Davie & Ratnoff.[4,5] Two different clotting systems existed, one being the extrinsic system while the other was the intrinsic (or glass activated) system. It was observed that patients with deficiencies in factors such as XI or XII did not hemorrhage like patients that were lacking VII, which was known to form a complex with TF.[1] When the TF-F.VIIa complex was shown to activate F.IX[6], a link between the two pathways of coagulation was recognized in which TF served as the primary initiator of coagulation. In 1998, the intrinsic and extrinsic pathways were combined, thus defining our current understanding of the clotting cascade[7] (Figure 2). An explosion of TF research occurred the year I was born, 1987, due to the molecule being sequenced independently by four different groups.[8,9,10,11] The story of TF has since been ever evolving.

B. The Coagulation Cascade

Blood coagulation happens when serine protease enzymes assemble on membrane surfaces with cofactors in a calcium-dependent manner.[12] Most coagulation proteins are synthesized as either zymogens of proteases, or inactive cofactors. In both instances, they require a proteolytic cleavage to become active. The proteins are denoted by Roman numerals and have the suffix "a" when they have been activated.[13] The physiologically relevant initiator of blood coagulation is the integral plasma membrane protein TF.[14]

The extrinsic, or TF pathway, begins when cellular damage occurs and TF is exposed to the coagulation factors in the plasma. TF will then bind to F.VIIa, and acts as a cofactor to drastically increase F.VIIa proteolytic activity by as much as five orders of magnitude or more. The TF-F.VIIa complex, also called the extrinsic tenase complex, then either directly cleaves the F.X into F.Xa or acts on F.IX to produce F.IXa which, in the presence of its own cofactor F.VIIIa, will then cleave F.X (Figure 2).[15] The TF-F.VII-F.Xa complex can also activate F.VII to F.VIIa.[16]

The intrinsic cascade is initiated when blood contacts a negatively charged surface and leads to the activation of F.XII. F.XIIa can activate prekallikrein to kallikrein, which in turn can amplify the intrinsic cascade by activating additional F.XII. High molecular weight kininogen (HMWK) acts as a cofactor for F.XIIa and kallikrein, which can further amplify the cascade. F.XIIa will then activate F.XI and this leads to the activation of F.IX so it can form the intrinsic tenase complex with F.VIIIa. The intrinsic tenase complex will then activate F.X.[15,17,18]

The common pathway is where intrinsic and extrinsic cascades meet at the formation of the prothrombinase complex. F.Xa binds to its cofactor, F.Va, and this cleaves prothrombin into thrombin. Thrombin is the last protease in the cascade that ultimately cleaves fibrinogen into

insoluble fibrin strands to form a hemostatic plug. Thrombin can further amplify the cascade by activating cofactors V and VIII[17], and factor XI in the presence of activated platelets.[19]

Down-regulation of the cascade happens rapidly by tissue factor pathway inhibitor (TFPI) in a mechanism dependent on the presence of F.Xa.[2] The main source of TFPI is on endothelial cells with some amounts being present in plasma.[20] TFPI is a Kunitz-type protease inhibitor that forms a complex with F.Xa and will bind to the extrinsic TF-F.VIIa complex or, alternatively, interact with TF-VIIa-X(a) to halt coagulation.[20,21]

C. Expression Levels and Non-hemostatic Roles

TF expression is necessary to sustain life. Since no human diseases attributed to a loss of TF have been reported, it appears that the molecule is critical for normal function.[1] Studies have shown that TF knock-out in murine models have embryonic lethal phenotypes. Separate researchers have proposed that this was due to either fatal bleeding or it was due to improper formation of the yolk sack vasculature.[22,23,24] The latter suggests that the protein is important for embryonic blood vessel development independent of coagulation.[25] TF also plays an important role in angiogenesis for wound healing.[26]

TF expression is not uniform in tissues thought the body. Tissues that have low levels of expression include joints and skeletal muscle, as these areas rely on the intrinsic pathway for hemostatic protection, and explains why patients with hemophilia often bleed into soft tissues and joints.[25] TF is highly expressed around and within highly vascularized organs such as the brain (Figure 3), lungs, uterus, heart, kidneys, placenta, intestines, testes, body surfaces, and surrounding blood vessels .[2,27] Astrocytes within the brain have some of the highest expression

levels.[28] These areas of high expression provide protection by creating a hemostatic "envelope".[27]

Vascular cells, including the endothelium, do not contain detectable levels of TF under normal conditions. TF expression is regulated by gene expression, and procoagulant activity is regulated at the post-translational level. For example, TF can be transiently induced through transcription factors NF-κB and AP-1 under pathological conditions such as exposure to lipopolysaccharide (LPS).[29] Some cells that are capable of expression are neutrophils, eosinophils, monocytes, macrophages, and endothelial cells.[2] Monocytes can expel TF-positive microvesicles that can bind to other cells in circulation, including platelets, and make cell types in the vasculature become positive for TF.[2,30,31]

Inappropriate TF expression is often detected in disease states such as thrombosis, cancer, sepsis, and atherosclerosis. When atherosclerotic lesions burst they expose high levels of TF that can lead to thrombus formation.[32] In sepsis, there is crosstalk between inflammation and coagulation. TF expression can be widely induced, activating system-wide coagulation which can lead to life threatening disseminated intravascular coagulation.[33] In a number of cancers (e.g., pancreatic, colorectal, adenocarcenoma, breast, prostate, and brain)[34,35,36,37], it is common for TF to be aberrantly expressed and linked to angiogenesis, metastasis, and growth in tumors.[38] TF pathology can come from its ability to communicate with G coupled protease activated receptors (PARs). The TF-FVIIa complex can directly active PAR2, a receptor for trypsin[39], while the ternary complex (TF-FVIIa-FXa) can activate both PAR1, a receptor for thrombin[40], and PAR2, which leads to signal transduction.[41] This leads to a poorer prognosis

than in patients who do not upregulate TF. In cancer patients thromboembolism is a leading cause of death.[2]

D. Structure

In humans the TF gene is located on chromosome 1 at location 1p21.[42] The DNA sequence of TF contains six exons. The first exon is responsible for the translation initiation and propeptide. Exons two through five are for the translation of the extracellular domain, while exon six codes for the transmembrane and cytoplasmic domains.[12] An alternatively spliced bloodborne form exists called alternatively spliced TF (asTF). As opposed to full length TF, asTF is missing the fifth exon and exons four and six are spliced together. The resultant product produces a frameshift, producing a molecule that lacks the transmembrane and cytoplasmic domains.[43] asTF is missing part of the region that binds to FX therefore has reduced procoagulant activity.[2]

Full length TF is a 47 kDa transmembrane glycoprotein that is made of 263 or 261 (both of which are approximately equal in expression[15]) amino acids and contains three distinct domains. TF is a member of the cytokine class II receptor family.[12,44] The TF molecule has a short cytoplamic domain that is different from other cytokine receptors, however, the external domain is structurally similar. Cytokine receptors when activated are known to form dimers and induce cell signaling.[45] The protein shares structural homology with interferon receptors α/β, and γ in the extracellular domain.[44] Cytokine receptors are conserved through many species from trout to human. Pufferfish, an animal that has not developed cytokines, has a protein with a sequence similar to TF. It may be possible that TF is the founder gene for all class II cytokine receptors.[46,47] The N-terminus, residues 1-219, makes up the extracellular domain

and is composed of two fibronectin type III domains that join at an angle of 125 degrees.[12] This domain is where there is an interaction between TF and F.VIIa and F.X. This extracellular domain also contains three N-linked glycosylation sites.[46,11] Residues 220-242 from the transmembrane region anchors TF to the membrane. This membrane association promotes the binding of other coagulation factors containing a γ-carboxyglutamic acid (GLA) through a Ca^{2+} bridge. C-terminal residues 243-263 form the cytoplasmic domain which is involved in signal transduction and contains two phosphorylation sites at Ser253 and Ser258 (Figure 4).[12]

E. Procoagulant Regulation

There has been evidence that suggests low levels of TF exist in circulating blood, but this is either cryptic or inhibited and must be activated to induce coagulation.[2,48] There are distinct populations of TF on membranes that exist as either an activated form (decrypted) or exist in a non-coagulant form (cryptic). It is important to note that cryptic TF can still form a complex with F.VIIa, however it does not functionally bind substrates F.X/F.IX.[49] The majority of TF that is expressed on cell surfaces is in a cryptic state. [21,50,51] A study in 1992 concluded that OC-2008, a human ovarian carcinoma line, has less than 20% of TF molecules in an active state.[51] TF activity on several other examples of human cells can be seen in Table 1. HUVECs are primary human umbilical vein endothelial cells. Cell line WI-38 is of fibroblast origin, MDA-231 is from breast cancer, and THP-1 is from monocytes. Currently the mechanism underlying TF decryption remains a mystery.

There are many contradicting hypotheses about how the procoagulant activity of TF is regulated. Currently there are multiple ideas that predict the transformation of TF from non-coagulant to procoagulant, none of which have definitive supporting evidence. In fact, there

are discrepancies in the literature underlying each proposed mechanism. However, each of these mechanisms has one thing in common - post translational modification.

There are different mechanisms of post translational control of the procoagulant activity of TF. The most widely known is the rearrangement of phosphatidylserine (PS) on the membrane to concentrate F.VIIa and F.X on the cell surface to interact with TF; this is mandatory for optimal activity.[52] In quiescent cells there is phospholipid asymmetry where the neutral choline phospholipids, sphingomyelin and phosphatidylcholine, are in the outer leaflet. The inner leaflet contains the negatively charged phospholipids, PS and phosphatidylethanolamine. Once cellular activation has occurred there is a loss of asymmetry and the negatively charged phospholipids are able to flip to the outer leaflet. This facilitates binding of coagulation proteins with a GLA domain (prothrombin, F.VII, F.IX, and F.X) in a Ca^{2+} dependent manner.[2]

It was discovered that PS exposure is not the sole contributor to decryption, there is another underlying mechanism.[53] The organization of the membrane lipids into microdomains may contribute to the conversion of cryptic TF into procoagulant TF. There exist microdomains, or lipid rafts, in the outer leaflet that are rich in glycosphingolipids and cholesterol. These lipid rich regions are known to influence cellular events such as signal transduction, membrane trafficking, and protein-protein and lipid-protein interactions.[54] Such microdomains have been implicated in regulating the procoagulant activity of TF. One study conducted on HEK293 cells found that depleting cholesterol with methyl-beta-cyclodextrin increased procoagulant activity. The mechanism behind this is that disruption of lipid microdomains led to mis-regulation of the enzyme that normally restricts anionic phospholipids to the inner leaflet, increasing their availability to the TF-F.VIIa complex .[55] However there are also contradicting results as another

study has found that depleting membrane cholesterol in WI-38 cells decreased the procoagulant activity of TF by reducing the binding of F.VIIa .[56]

Another potential mechanism of TF decryption is through glycosylation of the N-linked glycosylation sites, however this appears to be membrane dependent as no effects were seen with soluble TF. Glycosylation of proteins provides many essential roles in biological function, such as regulating signaling and structural changes.[57] A study by Krudysz-Amblo et al. found that human placental TF had more glycosylation and heterogeneity in its sugar moieties than recombinant TF.[58] A mutational study done to disrupt the Cys186-Cys209 disulfide bond to decrease activity of TF also decreased glycosylation.[59] The Asn-124 glycosylation site in TF is near the Cys186-Cys209 disulfide bond and the F.X recognition site, and its glycosylation state could affect TF activity.[58] However there are contradicting results, as another study concluded that there was no difference in TF activity between wild type TF and TF mutants lacking N-linked glycans in transduced human endothelial cells or Chinese hamster ovary cells.[60]

While the modifications of TF described above have been proposed to influence TF activity, there are two main competing hypotheses proposed to explain regulation of TF procoagulant activity. One hypothesis, the allosteric disulfide bond hypothesis, proposes decryption through regulation of the redox state through an allosteric disulfide bond (Figure 5). There are two disulfide bonds in the TF extracellular domain: Cys49-Cys56 and Cys186-Cys209. One study demonstrated reduced activity when a mutation was introduced to either the Cys186 or Cys209; however, no effect was seen when a mutation was introduced to either Cys49 or Cys57.[59] This suggested that the Cys186-Cys209 disulfide bond was important for the activation of TF. Protein disulfide isomerase (PDI) is proposed to be an important mediator of the redox

state of TF.[61] When the thiols are oxidized the molecule has procoagulant activity, whereas when the bond is reduced the activity is decreased. There are few contradictions surrounding this hypothesis. PDI can also influence the exposure of PS, and it has not yet been proved that there are free thiols in vivo.[2,21] The disulfide bond must be in an oxidized state before TF can form a complex with F.VIIa, and according to Bach and Monroe[62], F.VIIa is already bound to all available TF in and surrounding the vasculature, therefore PDI cannot be responsible for decryption. Another matter is that not all cell types show TF regulation by thiol exchange, such as cancer cells that constitutively express active TF.[63]

An alternative to the allosteric disulfide bond hypothesis is the TF self-association hypothesis. Chemical cross linking studies have shown that approximately 40% of TF exists as multimers and dimers on resting HL-60 cells, and activation of the cells abolishes self-association of TF.[64] Key components in the self-association of TF molecules are the cytoplasmic and transmembrane domains because they promote TF localization to lipid rich microdomains and are proposed to keep them cryptic through contact interactions between TF molecules, respectively.[49] It is believed that at the interface of the TF homodimers there is a docking site for F.X/F.IX that is blocked when the molecules form multimers (refer to Figure 1).[21,49] There are contradictions associated with this hypothesis as well. For example, cross linking studies have not demonstrated that TF quaternary structural changes are responsible for a change in function[64], and TF dimers and oligomers have not been observed in some cell types.[52] An additional study with engineered dimers of the TF extracellular domain concluded that dimerization did not delay F.Xa generation.[65] The behavior of solution-phase TF is not expected to be exactly the same as membrane bound TF. If TF in solution can activate F.X this may be due

to a lack of steric hindrance because TF molecules can move more freely in solution than when membrane bound.[49] We have evaluated the self-association hypothesis in 300.19 cells stably transfected with TF using FRET to understand if oligomerization has an effect on the procoagulant activity of human TF.

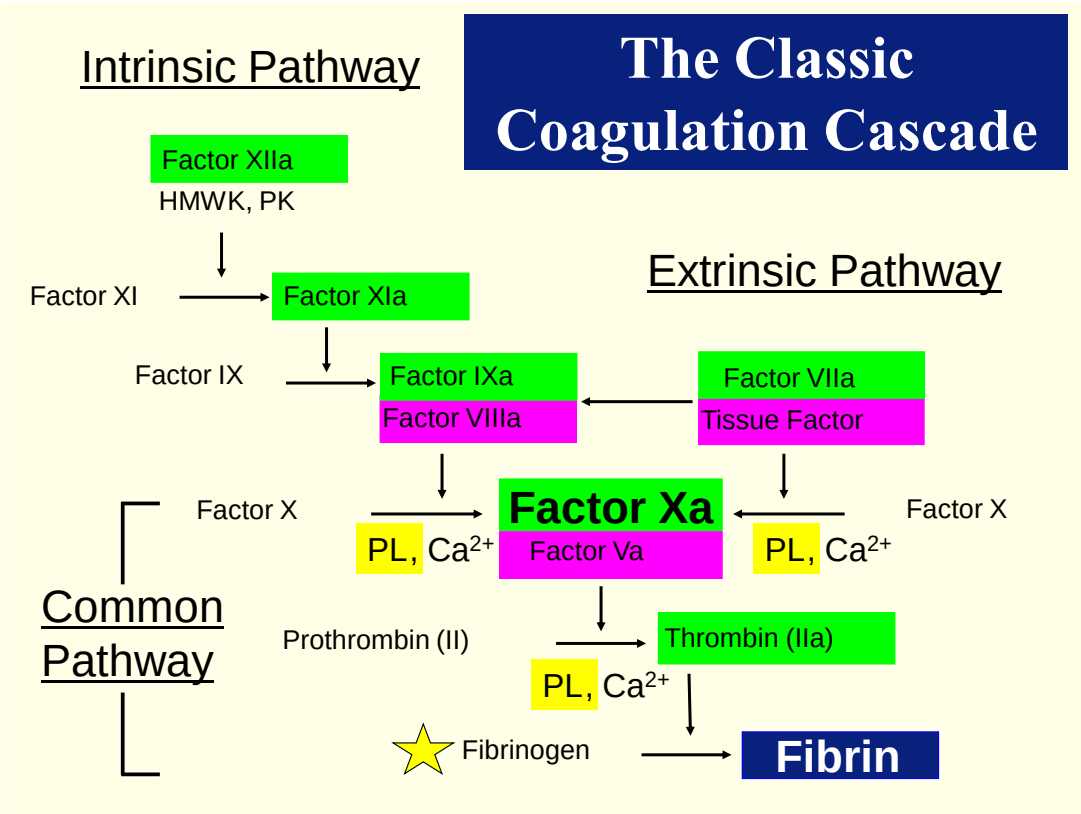

Figure 2: The classic coagulation cascade. In green are serine proteases, magenta are cofactors. PL represents negatively charged phospholipids and Ca^{2+} represents calcium, both of which are required for assembling complexes containing γ-carboxyglutamic acid (GLA)-domain proteins on the membrane. Star indicates terminal glycoprotein fibrinogen that polymerizes to insoluble fibrin once cleaved by thrombin.

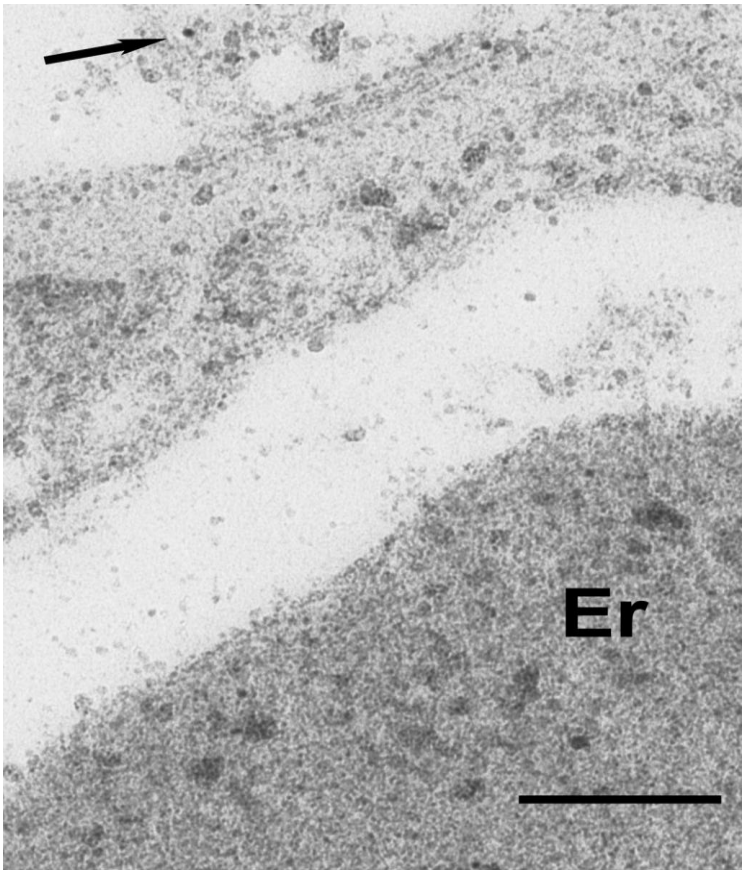

Figure 3: Immunogold localization of TF in murine brain seen in a transmission electron micrograph. Arrow indicates 10 nm gold nanoparticle that is outside of a capillary where TF is expected to be expressed. Er represents erythrocyte within the vasculature. Scale bar is 250 nm.

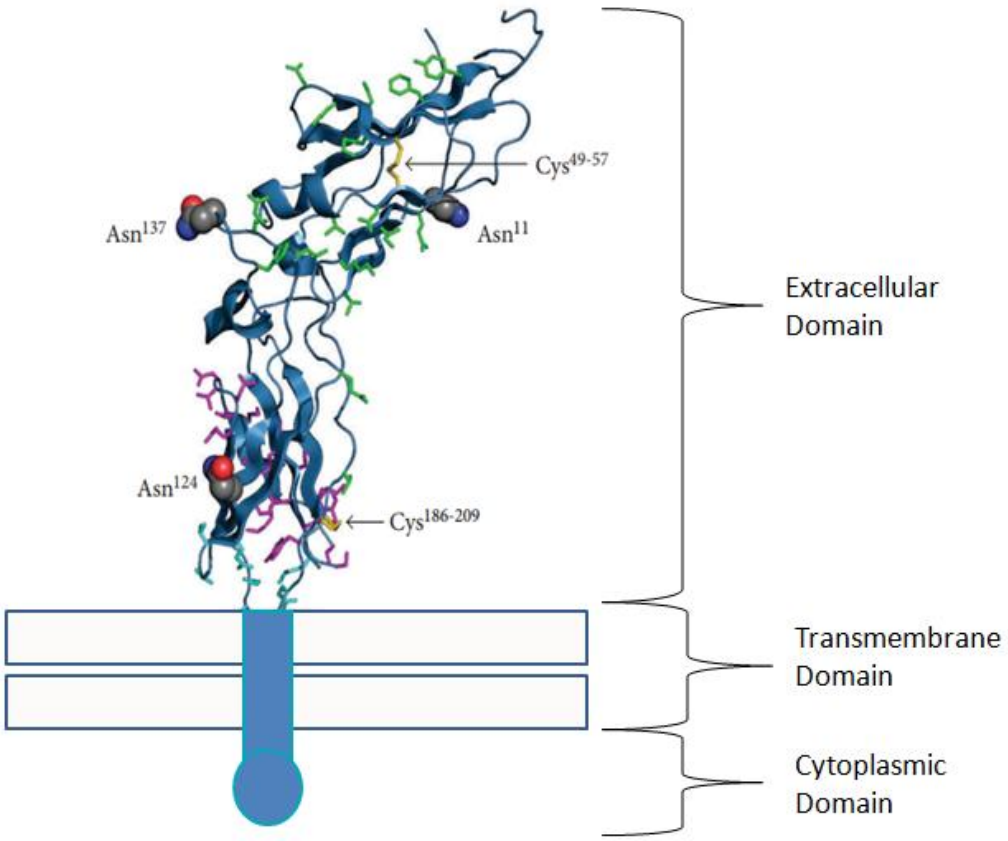

Figure 4: The structure of TF showing its three domains. The extracellular region can be glycosylated and/or modified through disulfide bonding, and contains regions where it makes interactions with F.VIIa and F.X. The areas in green are where it makes an interaction with the F.VIIa protease, and in pink is where F.Xa binds. Figure from Butenas.[12]

Cell Type	Cryptic %	Decrypted %	TF molecules/Cell	F.Xa generated (nM/min per fmole TF)
WI-38	83	17	2.70×10^5	0.058
MDA-231	79	21	11.23×10^5	0.016
Perturbed HUVEC	36	64	4.90×10^4	0.101
Perturbed THP-1	86	14	7.83×10^3	0.037

Table 1: Examples of the percentages of TF in a cryptic or decrypted state on various TF-expressing cell types. Most TF on cell surfaces remains in a cryptic state. There is one exception in the HUVEC cells that have most TF in an active form, most likely due to the fact that the cells had been stimulated with inflammatory mediators TNF-α + IL1-β. Even when stimulated by LPS, the majority of TF on THP-1 cells remained cryptic. TF molecules/cell are based on ^{125}I-F.VIIa binding. F.Xa generated for MDA-231 cells interestingly is the lowest despite having the highest amount of TF molecules/cell. The WI-38 cell line generated more F.Xa than the perturbed THP-1 but it is noted that the TF molecules per cell on the WI-38 line is two orders of magnitude more than the THP-1 line. The perturbed HUVEC cells produced the most F.Xa generation but this also had a higher percentage of decrypted molecules. Perhaps such variation is due to differences in cell membrane environments or other cellular machinery. Data obtained from Kothari, et al.[66]

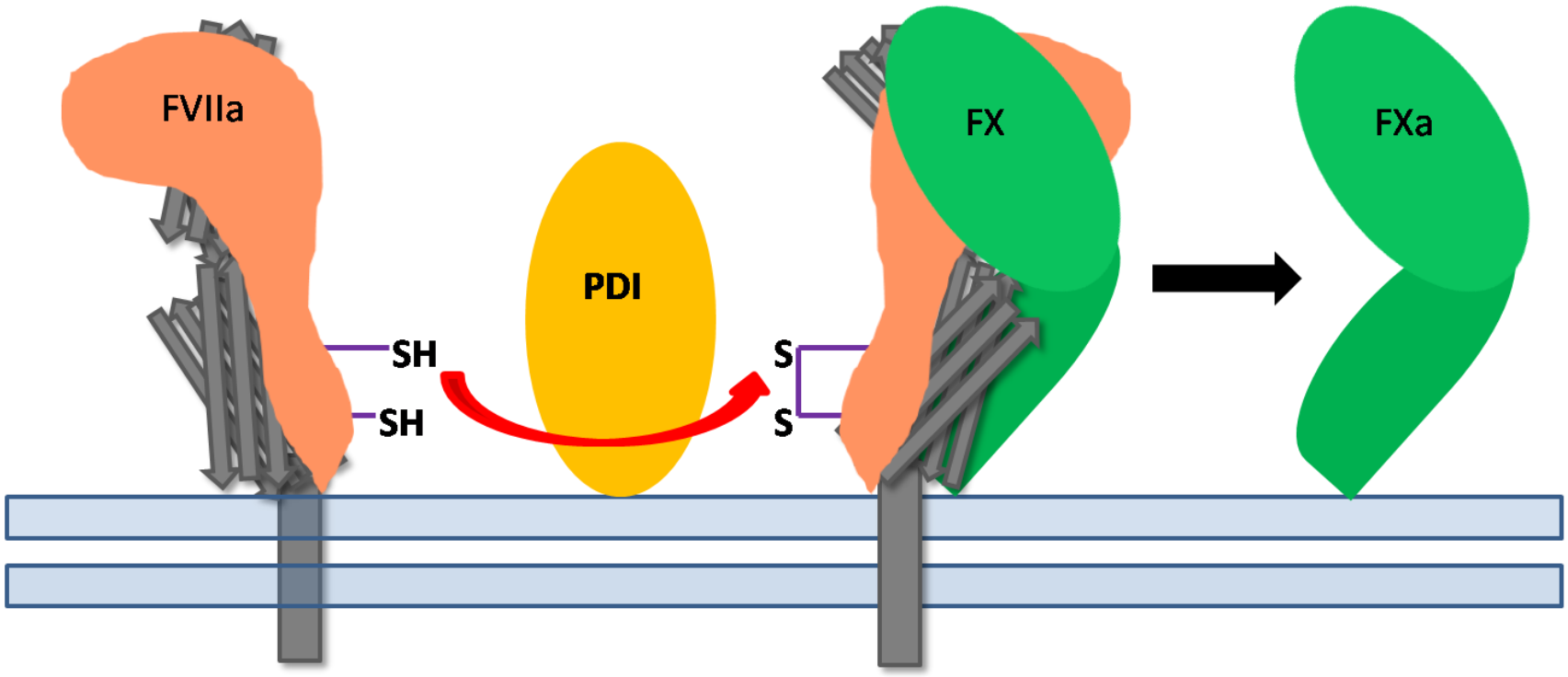

Figure 5: The allosteric disulfide bond hypothesis is one of the competing hypotheses that propose TF decryption. The redox state of the disulfide cys186-cys209 may be important by causing a conformational change that leads to decryption. Protein disulfide isomerase (PDI) is an important mediator of the redox state of the cys186-cys209 bond. When the disulfides are reduced TF is cryptic and once the bond is oxidized a conformational change occurs allowing for the activation of F.X.

III: Materials and Methods

DNA

Four different plasmids based on the parent pECFP-N1 (gift of P. Park, Case Western Reserve University)[67] that contain the two fluorophores of interest were used. The parent was modified by replacing the original cyan fluorescent protein sequence located 3' to the insert site with the relevant fluorophores, and by introducing a 1D4 epitope tag sequence at the 3' end of the fluorescent reporter sequence. Two of the plasmids contain sequence of our donor fluorophore, mTurqouise (mTq), one with the original full-length cytomegalovirus (CMV) promoter, and the other with a truncated CMV promoter that drives lower expression levels. The other two plasmids contain a super yellow fluorescent protein 2 (SYFP2) sequence, with the full-length and truncated CMV promoters. The plasmid DNA was purified with two different procedures. For screening, this was done with an alkaline lysis mini prep with reagents made in house. A QIAprep Spin Miniprep kit (catalogue # 27104) was used to isolate ultra-pure plasmid DNA for ligation and sequencing reactions. In brief, transformed *E. coli* were spun down and supernatant was discarded. 250µL of solution P1 was added to resuspend cells. 250µL of P2 was added to lyse the cells followed by the addition of 350µL of neutralization buffer N3. The mix was spun at maximum speed in a microcentrifuge for 10 minutes and supernatant was added to QIAgen spin columns and eluted with elution buffer. DNA concentrations were checked with a Beckman Coulter DU800 spectrophotometer at dilutions of 1:60.

PCR to Amplify Human TF

Human TF was amplified from a plasmid source (generous gift of L-C Petersen, Novo Nordisk, Måløv, Denmark), and HindIII and BamHI sites were added at the 5' and 3' ends, respectively.

The primers designed are as follows. Forward: 5’ ATA TAA GCT TGC CAC CAT GGA GAC CCC TGC CTG 3’; reverse: 5’ CTC GGG ATC CCG TGA AAC ATT CAG TGG GGA GTT C 3’. Five reactions were done at 20 µL each. Each reaction contained 10µL of 2X Phusion master mix (Promega), 1µL of template plasmid DNA diluted 1:100, 1µL of 10µM forward primer, 1µL of 10µM reverse primer, and lastly 6µL of DNAse-free H_2O. The machine used was a Bio-Rad DNA Engine Peltier Thermal Cycler, with 30 cycles [98° 10 sec., 45°C 30 sec., 72°C 1 min.].

Restriction Digests

Restriction digests were completed to obtain the correct compatible sticky ends on both expression vector and PCR product. The enzymes used were HindIII and BamHI (NEB catalogue # R014T and R0136, respectively). 1µL of each enzyme was added to 1.2µg DNA along with 2µL 10X 2.1 buffer (NEB catalogue # B7202S). The digests took place at 37°C for 2 hours. Products were run on 0.8% agarose gels, bands were cut out and DNA was repurified using a QIAquick gel extraction kit (catalogue # 28704).

Ligation and Confirmation of Sequence

Ligation reactions were performed with 1µL of 10X T4 ligation buffer (Promega), 1µL T4 ligase (Promega), 1µL linearized vector, 3µL insert, and 4µL DNAse free H_2O. The reaction was completed at room temperature for three hours. One construct was made and sequence was verified by University of Chicago Comprehensive Cancer Center and DNA Sequencing and Genotyping Facility to ensure there were no mutations introduced during PCR. The TF cassette was generated in one of the four plasmids, then shuttled into the other three using the HindIII and BamHI sites after the correct sequence was confirmed.

Transformation

Novagen NovaBlue competent *E. coli* cells (catalogue # 70181-4) were transformed with 5µL of ligation reaction. Cells and DNA were incubated on ice for 15 min. followed by a 60 second heat shock at 42°C. The cells were transferred to ice for 2 min. 250µL of SOC medium was added to allow the cells to recover. The cells were then incubated at 37°C for one hour on a shaker at 200 RPM. 10µL of cells were plated on LB agar with 50µg/mL kanamycin and incubated overnight at 37°C. Colonies were grown in 5 mL LB with kanamycin for 15 hours, and plasmid DNA was purified with a QIAprep Spin Miniprep kit.

Tissue Culture

300.19 cells[68] were cultured in RPMI 1640 medium, supplemented with 10% fetal bovine serum (FBS), 100U/mL penicillin + 100µg/mL streptomycin, 55µM 2-mercaptoethanol as a reducing agent, and 2mM L-glutamine (complete medium). For selection of cells transfected with TF, complete medium was used with the addition of 1mg/mL G418. They were cultured at 37°C in 5% CO_2. Cell stocks were frozen in 10% DMSO in FBS.

Transfection

Plasmids were linearized with AseI (Promega) to prepare for transfection of mammalian cells. Reactions containing 5µg DNA and 1µL AseI were incubated for 2 hours at 37°C. DNA was repurified using the QIAquick gel extraction kit. Cells were then washed in basal medium with 20mM HEPES before transfection to remove residual proteins. 5µg of linearized DNA along with 2×10^6 cells were added to an electroporation cuvette with 0.4cm gap (BioRad). The cuvette was placed on ice for 10 minutes, then transferred to the electroporator (BioRad GenePulser Xcell) and a pulse of 280V, and capacitance of 950µF using exponential decay was discharged into the cell suspension. The cells were then added to a T25 flask with complete medium to a

total volume of 10 mL. After an overnight recovery period, G418 selection agent was added to a final concentration of 1 mg/mL. After 12 days of selection, the cell suspension was pelleted through 1 mL FBS to remove debris and returned to culture in 10 mL complete medium with G418.

Single Cell Cloning

After 12 days of selection from transfection, a 10-fold dilution series of cells was made and plated at approximately 200µL of each dilution into individual wells in 96 well plates. Individual colonies of cells were transferred to 24 well plates followed by transfer to T25 flasks with complete medium and 1 mg/mL G418. Clones were grown to approximately 2-4 x 10^6/mL. Freezer stocks were generated, and the remaining cells were prepared for flow cytometry and fluorescence microscopy analysis.

Labeling for Flow Cytometry/Fluorescent Microscopy Analysis

Labeling was perfomed on 0.5 X 10^6 cells per test. All labeling procedures were carried out on ice to prevent internalization of the antibody through its crosslinking of membrane proteins. Cells were aliquoted into 12 X 75 mm polystyrene tubes, and washed twice with phosphate buffered saline (PBS) + 2% horse serum (wash buffer). Nonspecific binding was blocked with PBS + 5% normal goat serum (NGS) for 15 minutes. The cells were incubated with 50µL (final concentration of 5µg/mL) of mouse anti-human tissue factor (BD Pharmingen catalogue # 550252) in wash buffer for 30 minutes. The cells were washed twice with wash buffer. The cells were then incubated with 50µL goat anti-mouse IgG (H+L) conjugated to Alexa Fluor 647 (Southern Biotech catalogue # 1036-31) or TRITC (Southern Biotech Catalogue # 1030-03) at a final dilution of 1:200 for 30 minutes. After the samples were washed twice with wash buffer,

they were fixed in 1.5% formaldehyde in PBS. Flow cytometry analysis was done on a BD FACSCalibur flow cytometer to quantitatively evaluate the surface expression levels. Fluorescent images were also taken to qualitatively visualize cells and their levels of TF expression.

FRET Measurements

Cells were harvested and pelleted in a tabletop centrifuge for 5 minutes at 1400 RPM. Medium was aspirated and the cells were resuspended in 1mL complete medium with 1mg/mL G418. In the biophysical microspectroscopy facility, cells were pelleted and resuspended in approximately 50 µL HEPES buffered saline (HBS) (150 mM NaCl, 20mM HEPES, pH 7.4, supplemented with 5 mM Ca2+) and a wet mount was made with 10µL of solution. Wet mounts were imaged at room temperature with a Nikon Eclipse two-photon microscope using a 100X magnification oil immersion objective lens and OptiMiS scanning/detection head (Aurora Spectral Technologies, Grafton, WI). We obtained spectrally resolved fluorescence images with excitation from a mode-locked MaiTai Ti: Sapphire laser that was tuned to 815 nm to excite our donor, and 930 nm to excite our acceptor. Emitted fluorescence was collected passing through a transmission grating onto a cooled electron-multiplying charge coupled-device camera that has single photon sensitivity (iXon X3 897, Andor Technologies, Belfast, UK).

Some samples were tested in the presence of varying concentrations of ligand F.VIIa (2.5nM, 5nM, or 10nM, Enzyme Research Laboratories catalogue # HFVIIa 5120). To assess FRET in the absence of trace F.VIIa from the culture medium, another set of samples was prepared by washing in HBS with 10 mM EDTA and then allowed to recover in the presence of $Ca2^{+}$. To assess the effect of cell activation on FRET, the cells were stimulated with either

phorbol myristate acetate (PMA, Biomol International catalogue # PE-160) or lipopolysaccharide (LPS, *E. coli* strain O111:B4, Sigma-Aldrich catalog #L4391). PMA at 60ng/mL in HBS supplemented with 5mM Ca^{2+} was added to the cell pellet. Samples were incubated for 30 min. at room temperature before being imaged. LPS-activated cells were cultured in 1µg/mL for 18 hours before imaging.

FRET Analysis

Spectral imaging was done on the single transfectants to obtain the control emission spectra for both donor and acceptor. Emission spectra was obtained from cells expressing mTurquoise (mTq) at a wavelength of 815 nm or separately, super yellow fluorescent protein 2 (SYFP2) at 930 nm. These spectra were averaged and normalized according to maximum intensity to create elementary spectra. Spectral images of dually transfected cells were examined and unmixed at the pixel level to determine the donor fluorescence intensity in presence of acceptor (k^{DA}) and the acceptor fluorescence intensity in presence of donor (k^{AD}) for every pixel of the imaged section of the cell.[69,70] Since we are only interested in membrane TF, we selected regions of interest (ROI) that includes pixels from the surface membrane and excludes them from other membrane compartments of the cells such as endoplasmic reticulum. Histograms showing the distribution of FRET efficiency across pixels within a segment were created, and the dominant peaks in these histograms were then assembled into meta-histograms to determine the dominant quaternary structure of the oligomers. The programs used were written in house by the Raicu group using Matlab programming language.

TF Activity Assay

Cells were harvested and pelleted, then washed 3X in HBS with 0.1 % bovine serum albumin (BSA) and 2mM Ca^{2+}, then once in HBS/BSA with 10 mM EDTA to remove residual clotting factors from the serum-containing media. They were then washed twice with HBS/BSA with 2 mM Ca^{2+} to allow recovery. The cell count was adjusted to 0.75 x 10^6/mL and 1.5 X 10^5 cells were added to 96 well round bottom plates in a volume of 200 µL. Reaction or control mixtures were added in 60µL volumes. Reaction mixtures contained reagents to deliver final concentrations of 135nM F.X (Haematologic Technologies catalogue # HCX-0050), 0.2nM F.VIIa (Enzyme Research Laboratories catalogue # HFVIIa 5120), 3mM Ca^{2+}, and buffer to volume. Controls excluded either F.X to test specificity of the Xa chromogenic substrate, F.VIIa to test for residual F.VIIa from serum-containing media, or Ca^{2+} to test for biological relevance. Samples were incubated for 1 hour at 37°C in a sealed plate. Cells were pelleted after the incubation, and 40µL supernatant was transferred to a fresh 96 well round bottom plate containing 40µL ice-cold HBS/BSA/EDTA per well to stop the reaction. The amount of F.Xa generated during the incubation was measured by adding 20µL chromogenic substrate Spectrozyme FXa (Biomedica catalogue # 222L) at a final concentration of 1.25 mM. Activity was monitored as a kinetic read at 405 nm for 30 minutes in a microtiter plate reader (VersaMAX, Molecular Devices). The rate at which the yellow product appears is proportional to the amount of F.Xa produced by TF-F.VIIa complexes during the incubation at 37°C. Data collection and analysis were performed with SoftMAX software, using the maximum mOD/min. of *p*-nitroaniline released from the chromogenic substrate.

IV: Results

A. Tissue Factor Fusion Protein Constructs

To carry out hypothesis testing we created fusion proteins to evaluate TF expression and function. All four plasmids initially contained the gene that encoded rhodopsin. The rhodopsin gene was removed with digestion of HindIII on the 5' end and BamHI on the 3' end, to be replaced with the TF gene. For this, an appropriately modified TF insert was amplified by PCR using a pcDNA3 plasmid containing the full-length human coding sequence as template. We designed PCR primers to introduce the necessary restriction sites at the 5' and 3' end, remove the stop codon, insert a Kozack consensus sequence for ribosome binding at the 5' end, and add a linker region on the 3' end. A plasmid map of our final product to create fusion proteins is pictured in Figure 6 A, and a map of the original plasmid that contained the TF gene is pictured in Figure 6 B. These plasmids were linearized and 300.19 cells were transfected and selected.

B. Transfection and Subcloning Results

The 300.19 cell line[68] makes an exquisite model for studies of TF. They are an immortal cell line, grow rapidly (Figure 7) and easily take up foreign DNA. They are a murine pre-B lymphocyte line, and having a vascular origin, are not expected to express our antigen of interest. In previous studies, we were unable to detect antigen with antibodies against human or mouse TF. When TF activity on 300.19 cells was compared to THP-1, a human cell line with inducible TF activity (Figure 8), we observed no signal above baseline with either mouse or human F.VIIa.

As expected the initial selection after transfection produced a heterogeneous population of TF-expressing cells (Figure 9). Single cell cloning enriched some lines for uniform

or relatively uniform expression. Some cells were subcloned a second time to further enrich cell for homogenous expression; an example of this can be seen in Figure 10. Through these methods, we have generated a library of cell lines that includes 300.19+TF+mTQ and 300.19+TF+SYFP2 single transfectants, and 300.19+TF+mTQ+SYFP2 double transfectants. In our initial experiments, we were unsure of whether high or low expression would give optimal results in FRET measurements. For this reason, our library includes cells transfected with donor and acceptor pairs under control of both full-length and truncated CMV promoters. Stable lines were successfully isolated when either the full-length or truncated CMV promoter was used to drive expression. The untagged TF lines express less TF than our fusion lines. This could possibly be due to the pcDNA3 plasmid itself. As an earlier generation of mammalian expression vectors, it has less optimization than do more recent products. For example, there are fewer base pairs in the pECFPN-1 and plasmid size known be inversely proportional to transfection efficiency.

Unfortunately, not all of the lines express TF-fluorophore fusion proteins in amounts that were easily detected in the fluorescent microscope. Therefore, we concentrated our efforts on lines that were found to be TF-positive by rapid microscopy screening. Example data selected from some of the 78 stably transfected TF-expressing cell lines in our library are reported in Tables 2-6. We have labeled select lines with an anti-TF antibody to look for distinct expression levels. We used the highest expressing lines for FRET experiments. Fluorescence images of these three cell lines can be seen in Figure 11, and quantitative MFI flow cytometry histograms can be seen in Figure 12. We have also generated a library of lines transfected with untagged TF, 300.19+HuTF, to use as a positive control in activity assays to determine if fusion proteins impact the ability of TF-F.VIIa to generate F.Xa (Table 6, Figure 10).

C. FRET Results

FRET is a sensitive technique that is used to test interactions of molecules less than 10nm apart.[71] This occurs due to non-radiative energy transfer between donor and acceptor molecules.[71,72] When fluorescently tagged proteins are within 10nm, the energy can be transferred through dipole-dipole interactions of the donor and acceptor, and this useful technique has allowed us to investigate whether TF self-associates.

We have used a two-photon microscope with spectral resolution to examine apparent FRET efficiency, $E_{app,}$ based on whether the donor fluorophore, mTurquoise (mTq), excites the acceptor fluorophore, super yellow fluorescent protein2 (SYFP2). The donor and acceptor fluorophores were chosen because there is a sizeable overlap in donor emission and acceptor excitation in the spectrum, and it is important that acceptor molecules are only excited by FRET as opposed to acceptor direct wavelengths. An example of the elementary spectra for both mTq and SYFP2 with single photon excitation and two-photon excitation can be seen in Figures 13 & 14, respectively. The stably transfected cell line 300.19+TF+mTq+SYFP2 10.3 was used to carry out these experiments by measuring the apparent FRET efficiency on both resting and stimulated cells.

A distribution map of E_{app} was created in the analysis programs using the equation[73]:

$$E_{app} = \frac{1}{1+\left(\frac{Q^A \; k^{DA} \; w^D}{Q^D \; k^{AD} \; w^A}\right)} \qquad (1)$$

where w^D and w^A are integrals of the normalized donor and acceptor spectra respectively,[71] Q^D = 0.84 is the quantum yield of mTq, Q^A = 0.68 is the quantum yield of the SYFP2[74], k^{DA} represents donor fluorescence intensity in presence of acceptor and k^{AD} represents the

acceptor fluorescence intensity in the presence of donor. From the calculated E_{app} we have demonstrated that FRET is occurring, and TF does oligomerize in small amounts (Figure 15). E_{app} histograms have been configured using values from hundreds of cells and thousands of regions of interest. Histograms were assembled into meta-histograms to evaluate the prominent peak positions and from these data it was determined that the quaternary structure of TF in the 10.3 cell line is primarily dimeric (Figure 16).

A pilot study was conducted by evaluating when different concentrations of F.VIIa were added to address whether or not ligand has an effect on the oligomeric state of the TF molecules. Concentrations of ligand added were 2.5nM, 5nM, 10nM, and 0nM (control) with EDTA wash to remove trace amounts of F.VIIa present in serum-containing media. Under these conditions, addition of FVIIa does not have a measurable effect on quaternary structure as there is still one peak in the meta-histograms, meaning E_{app} was similar in the resting 10.3 line, cells with EDTA wash, and cells that received different concentrations of ligand F.VIIa (Figure 17). Unexpectedly, there was a small shoulder to the left in the peak on the meta-histograms of the 5 nM F.VIIa compared to the resting 10.3 line. This is most likely because the 5 nM samples were the first tested and they were left concentrated while donor, acceptor, and 10.3 cells were imaged. For all other samples, the cells were harvested and immediately imaged. It is possible that the cells were starting to lose viability and this had an effect on the results. If 5 nM F.VIIa truly had an effect, we would have expected to see a similar effect with the 10 nM concentration as well.

Two cell activating agents have been used in this study. We used lipopolysaccharide (LPS) for slow stimulation that requires new protein synthesis, and phorbol myristate acetate

(PMA) for a faster, direct method of activation that bypasses surface receptors. It is interesting to note that the application of PMA stimulating agent can cause cells to shed microvesicles (Figure 18). The shedding of TF-positive microvesicles has pathological implications; if bound to TF negative cell surfaces within the vasculature events such as these could elicit unwarranted coagulation events as they could promote inappropriate coagulation elsewhere in the vasculature. In this study one example of a cell was analyzed using two wavelengths 815 nm and 930 nm to calculate average E_{app} in each ROI examined. Based on this analysis the average FRET efficiency per ROI was higher in the microvesicle region as compared to the cell from which they were presumably shed. No firm conclusion can be made since this is just one representative example and many more would need to be analyzed to do so. However, it is a noteworthy observation due to the potential for circulating microparticles with procoagulant TF to contribute to thrombosis.

To test our hypothesis that TF exists as oligomers on quiescent cells and upon stimulation, oligomers will dissociate leaving the protein fully active to initiate coagulation, we applied activating agents to dually transfected cells and measured FRET efficiency. If cell activation events that lead to TF decryption involve dissociation of oligomers, we expected to observe a decrease in $E_{app.}$ Upon cell stimulation with either PMA or LPS, our results show no decrease in apparent FRET efficiency. We can see these data in presented meta-histograms and the bar graph in Figure 19.

D. Activity Assay

It is assumed that the attachment of a reporter protein has no direct impact on the function of molecules. Our model is unique because we have a way to test the activity of cell

surface TF in cells transfected with and without fluorphores fused to the molecule. We have examined the activity of TF by measuring its ability to support F.Xa generation using a chromogeneic substrate. We have used a cell line without a fluorophore for a control, and a line that has a fluorophore attached to the protein to compare activity. It is vital to make sure the levels of surface expression of TF are approximately the same on the lines with and without the fluorophore for accurate comparative results. After flow cytometry analysis was complete we found two cell lines with approximately matching MFI. The cell lines that exhibited near matching levels were 300.19+TF+tmTq 9 and 300.19+huTF+1.6.3 (Figure 20 A). Our limiting factor in the activity assays was the lines with untagged TF. They all had much lower expression than the homogenous fusion protein lines created. We were able to utilize one of the mTq lines with the truncated CMV promoter because it exhibited lower expression than most of the homogenous fluorophore-tagged lines created (Table 4, Alexa Fluor 647 MFI values).

Three controls were used in activity assay experiments: no Ca^{2+} to test for the ability of procoagulant complexes to assemble, no F.VIIa to test for removal of residual F.VIIa by the EDTA wash, and no F.X to test the specificity of chromogenic substrate Spectrozyme FXa. The 300.19+TF+mTq+SYFP2 10.3 line used in FRET experiments was also tested side-by-side with fluorophore line tmTq 9 and non fluorophore line HuTF 1.6.3. The purpose of adding this cell line to the assay was to compare two lines with relatively low expression levels to one of the highest expressing lines to examine differences in total F.Xa generation, along with using this line for the controls (no Ca^{2+}, no F.VIIa, and no F.X).

No significant difference in F.Xa generation was observed between the tmTq 9 line and the 1.6.3 cell line, demonstrating that the addition of a fluorophore to the C-terminus of TF has

no effect on its procoagulant activity. Unexpectedly, the 10.3 cell line with far greater surface expression of TF, supported F.Xa generation to a level approximately equal to that on the tmTq 9 and 1.6.3 cell lines (Figure 20 B).

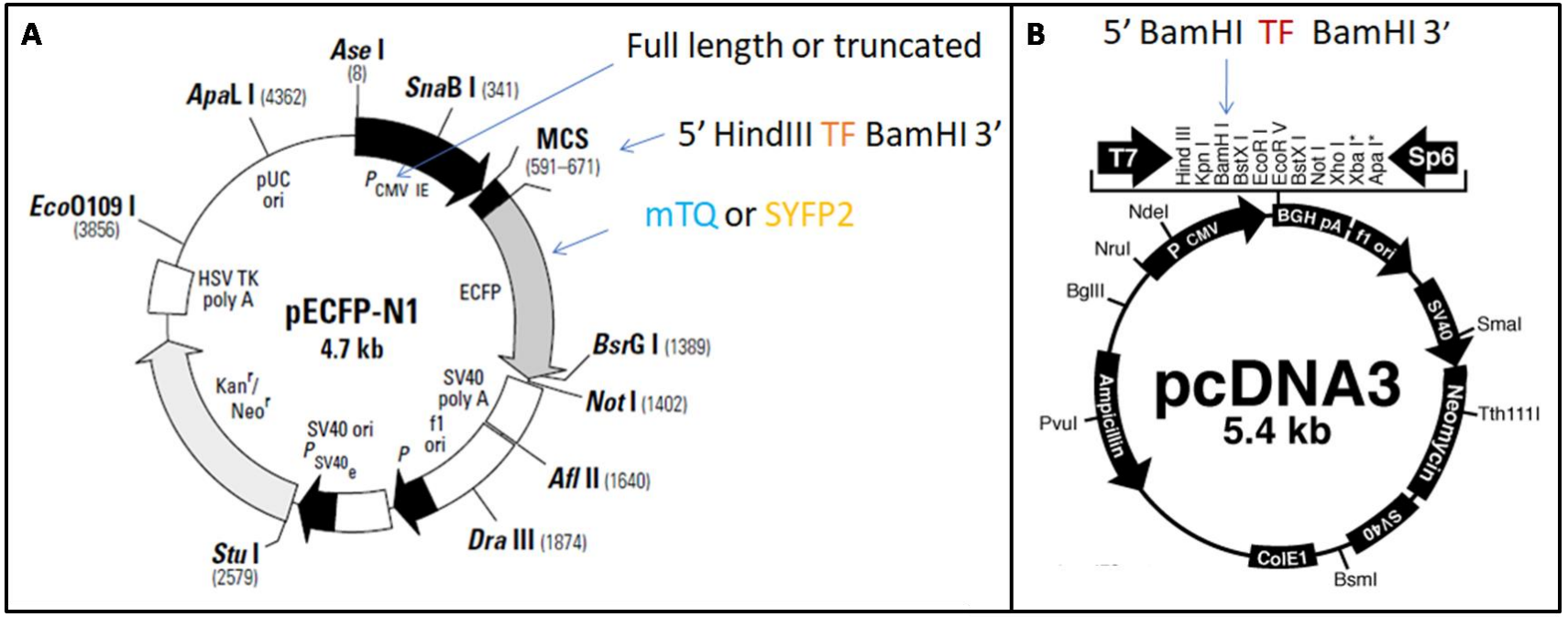

Figure 6: DNA constructs used for transfection. A. Diagram of the plasmid variants used to create our fusion protein-expressing lines. Plasmids were linearized at the AseI site before transfection. B. Diagram of the plasmid containing the full-length human TF sequence. This plasmid was used to create lines expressing untagged TF, and to amplify the TF sequence for later insertion into the pECFP-N1 plasmid. Image A from qualityard.com, Image B from tulane.edu

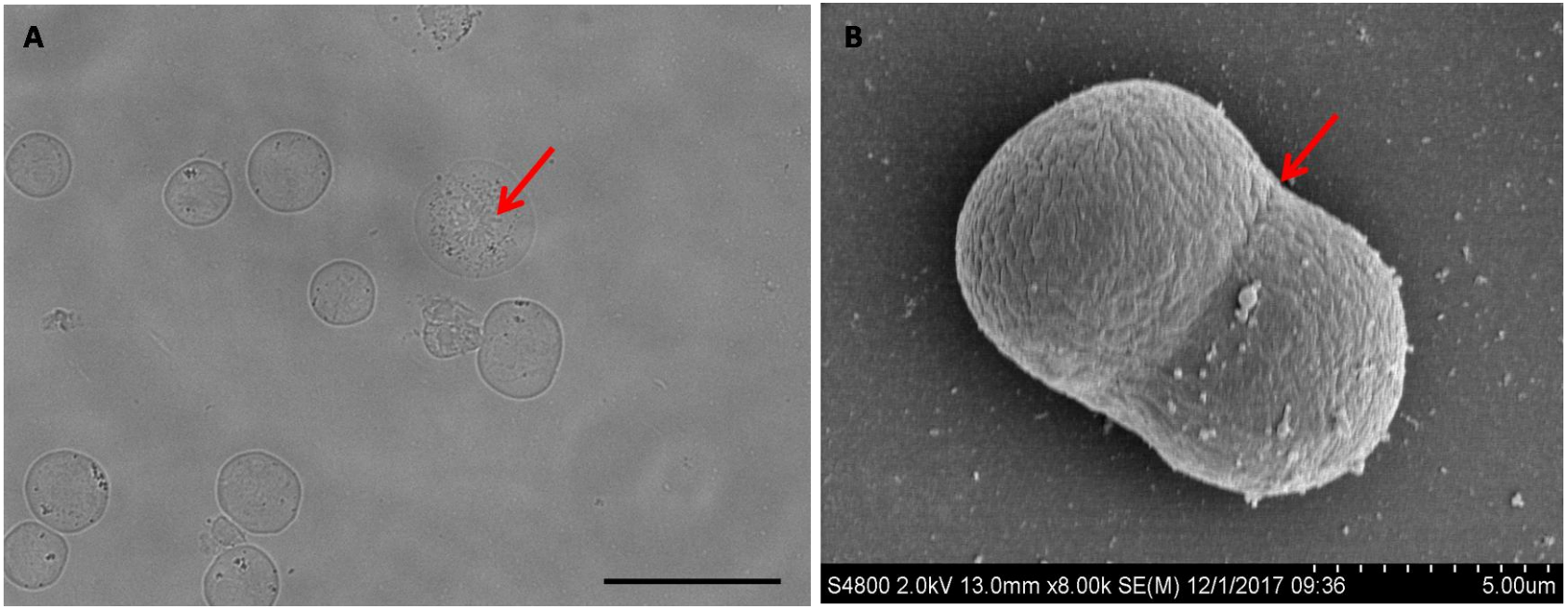

Figure 7: Rapid proliferation of 300.19 cells. Imaged are 300.19 cell undergoing two stages of mitosis. A. Bright field image of a cell in prophase seen by the large size of the cell and chromosomes condensing to prepare for cell division. Arrow indicates condensed chromosomes. B. Scanning electron micrograph of a 300.19 cell in cytokinesis. Arrow indicates cleavage furrow. Scale bar in A represents 25 µm.

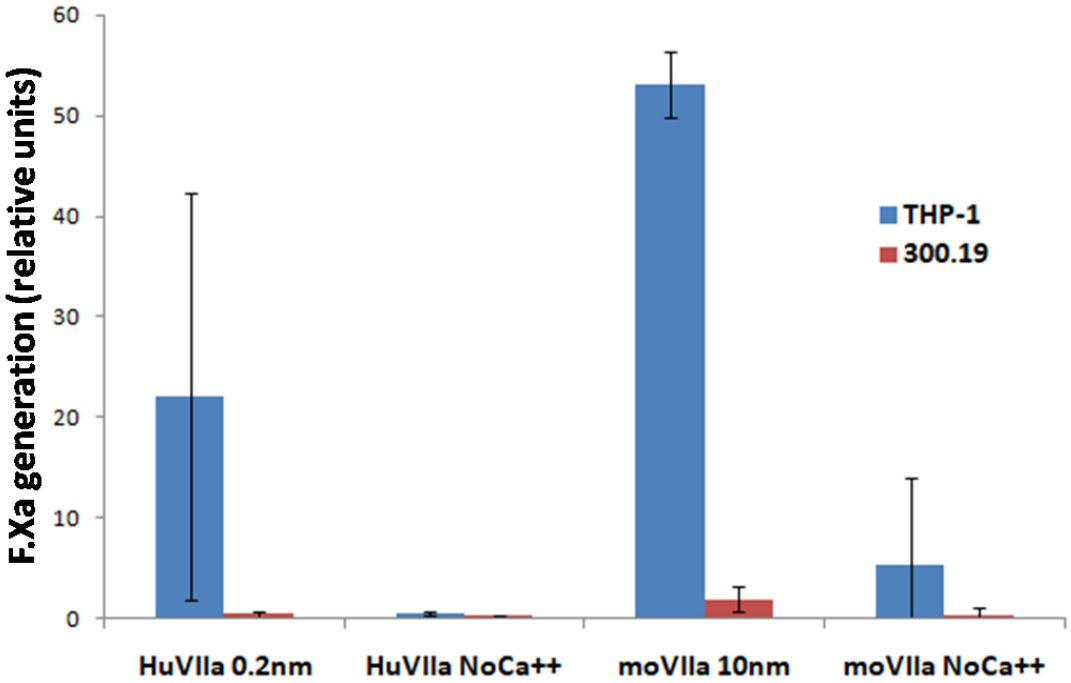

Figure 8: TF activity of THP-1 and 300.19 cell lines measured as F.Xa generation after LPS stimulation in the presence of Ca^{2+}, human or mouse F.VIIa and human F.X. Data were collected as a kinetic read at 405nm to measure the release of *p*-nitroaniline from a chromogenic substrate by the F.Xa generated. 25 points were used to calculate the maximum rate of color development, Vmax. The THP-1 cells have saturable TF activity, while the 300.19 cell line shows no activity above that of the negative controls (no Ca^{2+}).

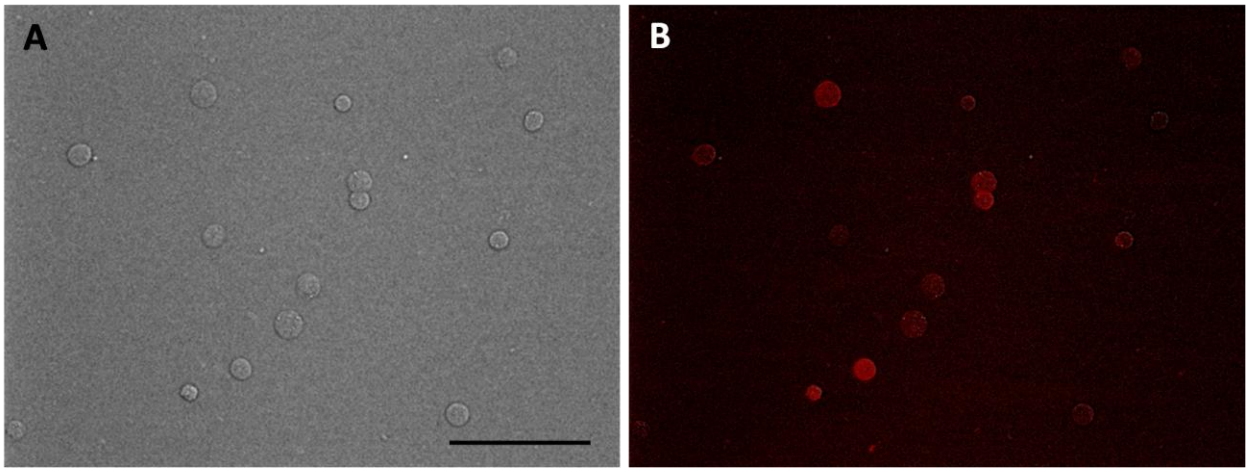

Figure 9: Representative image of initial heterogeneous cell population after transfection with untagged TF. A. Bright field image. B. Fluorescent image of anti-human TF monoclonal antibody and goat anti-mouse igG-TRITC detection. Some cells have far greater amounts of TF expression than other cells. Scale bar represents 50 μm.

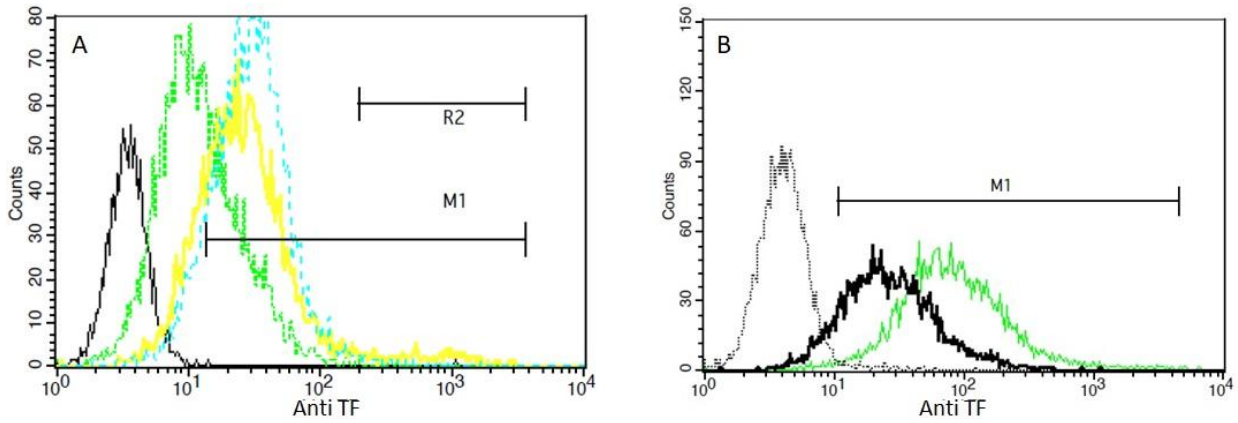

Figure 10: Flow cytometry fluorescence histograms of untagged TF expressing subclones with their respective levels of anti-TF antibody binding. A. The first round of subcloning showing different levels of expression can be observed. Black is the negative control and green, blue, and yellow, represent different subclones. The cell line in yellow, HuTF 1.6, has a significant population of cells with high TF expression (represented by R2) that suggests a subclone with uniformly high TF expression could potentially be isolated. HuTF 1.6 had a mean fluorescence intensity (MFI) of 45. B. Further subcloning of HuTF 1.6 enriched the population of high expressing cells. The thick black line and green line are two subclones of HuTF 1.6. The MFI of the HuTF 1.6.3 (green line) was 119 (2.6-fold increase). Dashed black line is the negative control.

Subclone	Average MFI	n	Distribution	Fluorescence microscopy
300.19+TF+mTq+SYFP2 1	31.45	2	Homogenous	Low mTq, not much SYFP2
300.19+TF+mTq+SYFP2 2	42.98	2	Heterogeneous	Moderate/Low
300.19+TF+mTq+SYFP2 3	28.69	2	Heterogeneous	No expression
300.19+TF+mTq+SYFP2 4	10.43	2	Homogenous	No expression
300.19+TF+mTq+SYFP2 5	33.39	2	Homogenous	Low<x<moderate levels
300.19+TF+mTq+SYFP2 6	9.93	2	Homogenous	No expression
300.19+TF+mTq+SYFP2 7	10.9	2	Homogenous	SYFP2 low, no mTq
300.19+TF+mTq+SYFP2 8	54.28	2	Heterogeneous	High/No expression
300.19+TF+mTq+SYFP2 9	28.02	2	Homogenous	Low levels of both
300.19+TF+mTq+SYFP2 10	32.67	2	Heterogeneous	High/moderate
300.19+TFmTq+SYFP2 10.1	51.4	1	Heterogeneous	High/moderate
300.19+TF+mTq+SYFP2 10.2	38.2	1	Homogenous	Moderately high
300.19+TF+mTq+SYFP2 10.3	95.13	2	Homogenous	High

Table 2: TF expression results for selected dual transfected clones with both fluorophores under control of the full-length promoter. These MFI results are obtained from indirect TF labeling and flow cytometry analysis while the fluorescent microscopy results come from qualitative screening. While all cells appeared to have relatively low expression, the 10.3 line contained the highest homogenous expression and was used in FRET experiments. <x< = between in tables 2-6.

Subclone	Average MFI	n	Distribution	Fluorescence Microscopy
300.19+TF+SYFP2 3	3	1	Heterogeneous	No visible fluorescence
300.19+TF+SYFP2 4	8.43	1	Heterogeneous	No visible fluorescence
300.19+TF+SYFP2 8	42.99	3	Homogenous	Moderate
300.19+TF+SYFP2 11	23.71	3	Homogenous	Moderate
300.19+TF+SYFP2 12	32.04	2	Homogenous	Moderate
300.19+TF+SYFP2 13	29.12	1	Homogenous	Low<x< Moderate
300.19+TF+SYFP2 14	54.45	3	Homogenous	High

Table 3: TF expression results for selected SYFP2 clones using indirect labeling. The SYFP2 8 clone, although not the highest expressing, was used as the acceptor control in FRET experiments because the cells grew much faster than the SYFP2 14 clones.

Subclone	Average MFI	n	Distribution	Fluorescence Microscopy
300.19+TF+mTq 1	3.98	2	Homogenous	Low
300.19+TF+mTq 2	30.94	3	Homogenous	Moderate
300.19+TF+mTq 4	32.7	2	Homogenous	Moderate <x< High
300.19+TF+mTq 5	38.1	4	Homogenous	High
300.19+TF+mTq 6	2.05	1	Heterogeneous	Low
300.19+TF+mTq 8	7.79	2	Heterogeneous	Moderate/High
300.19+TF+mTq 9	21.26	1	Homogenous	High

Table 4: TF expression results for selected mTq clones. The mTq 5 line was chosen as the donor control in FRET experiments because it has the highest expression.

Subclone	Average MFI	n	Distribution	Fluorescence Microscopy
300.19+TF+tmTq+tSYFP2	41.47	1	Homogeneous	High of both
300.19+TF+tSYFP2 1	39.24	1	Heterogeneous	Low
300.19+TF+tSYFP2 2	1.39	1	Heterogeneous	No visible fluorescence
300.19+TF+tSYFP2 3	2.35	1	Heterogeneous	No visible fluorescence
300.19+TF+tmTq1	4.33	1	Heterogeneous	No visible fluorescence
300.19+TF+tmTq 5	1.65	1	Heterogeneous	No visible fluorescence
300.19+TF+tmTq 9	18.11	3	Homogeneous	Very low

Table 5: TF expression results for selected truncated CMV promoter fusion proteins clones, denoted by t in front of the fluorophore. The tmTq 9 line was used in activity assays because it had an approximate match in the untagged TF lines that have lower expression levels.

Subclone	Average MFI FITC	n FITC	Average MFI Alexa	n Alexa	Distribution
300.19 +huTF 1.1	36.84	1	17.31	1	Homogeneous
300.19 +huTF 1.11	34.36	1	17.44	3	Homogenous
300.19 +huTF 1.12	26.58	1	8.55	3	Homogenous
300.19+huTF 1.6.3	116.76	1	19.58	3	Homogenous
300.19+huTF 1.6.4	77.42	1	9.73	1	Homogenous

Table 6: TF expression results for selected untagged TF clones. Tests were originally done with FITC conjugated secondary antibody to determine levels of expression. These data were used to identify lines with different levels of expression. Lines were then compared to fluorophore tagged lines using Alexa Fluor 647 detection. The 1.6.3 line was chosen for activity assays to compare to the tmTq 9 cell line (see Table 5). The HuTF 1.11 line would have been a desirable choice for further experiments, but it was lost in storage.

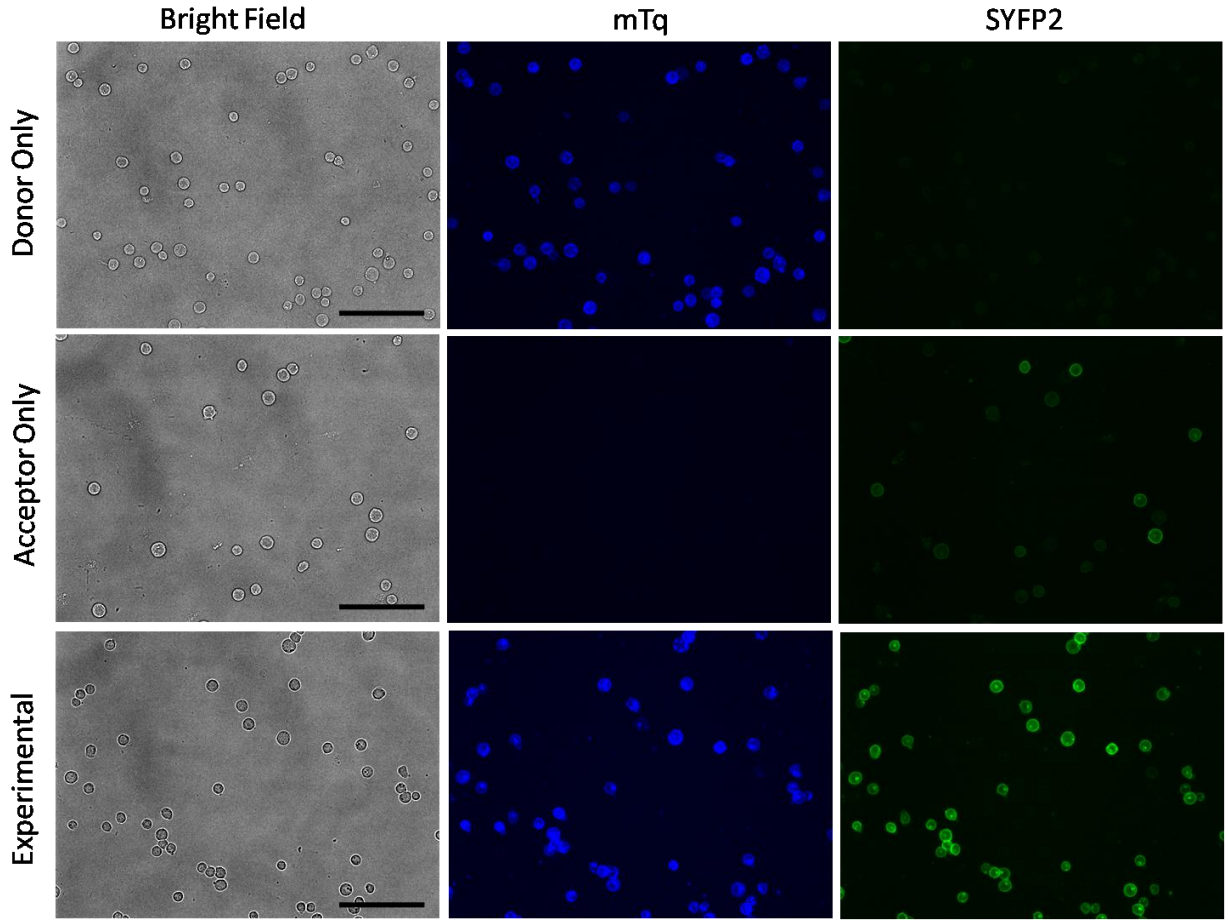

Figure 11: Representative fluorescence images of three cell lines created and used in FRET experiments taken at 200 ms exposure time. All lines showed fluorescence signal around the plasma membrane with some having a bright spot in the cell which is most likely endoplasmic reticulum. The Donor Only line is 300.19+TF+mTq 5, which yielded good elementary spectra by two-photon microscopy. The Acceptor Only line is 300.19+TF+SYFP2 8. This cell line had the lowest qualitative level of expression of the three lines analyzed. The Experimental line is dual transfectant 300.19+TF+mTq+SYFP2 10.3, this was used in FRET experiments and for activation and ligand studies due to the fact that it has the highest TF expression and grew at a fast pace. Scale bar represents 50 µm.

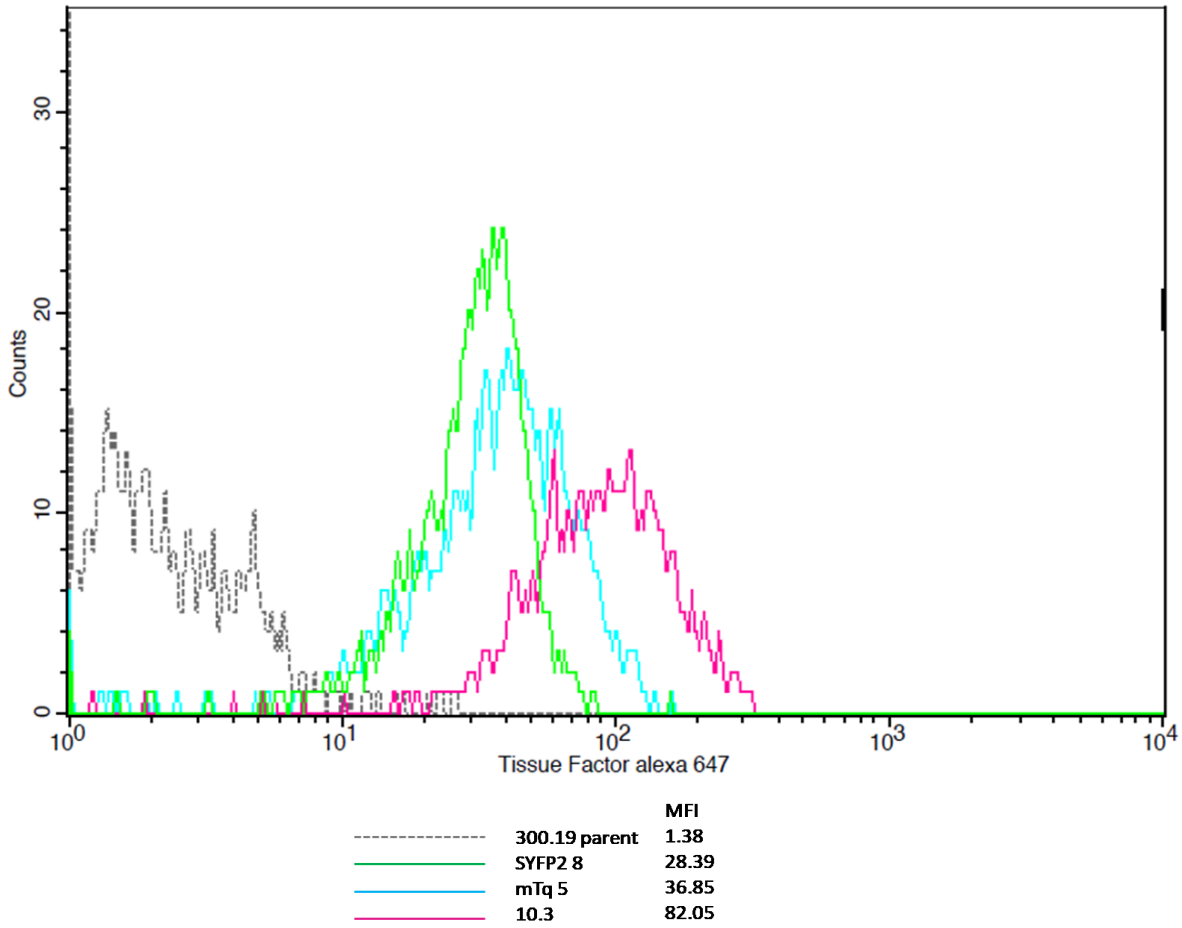

Figure 12: Quantitative flow cytometry histograms of cells used in FRET experiments after labeling with anti-TF monoclonal antibody and Alexa Fluor 647-conjugated secondary antibody. Consistent with images seen in Figure 10, the SYFP2 8 cell line has lower fluorescence intensity than the mTq 5 and 10.3 lines, indicating lower surface expression of TF. The dually transfected 10.3 line has a MFI approximately twice that of the single tranfectant lines, indicating about twice as much surface TF expression. Line 10.3 was used in subsequent FRET measurements. These results are based on one labeling experiment. Multiples experiments were conducted to obtain an average MFI.

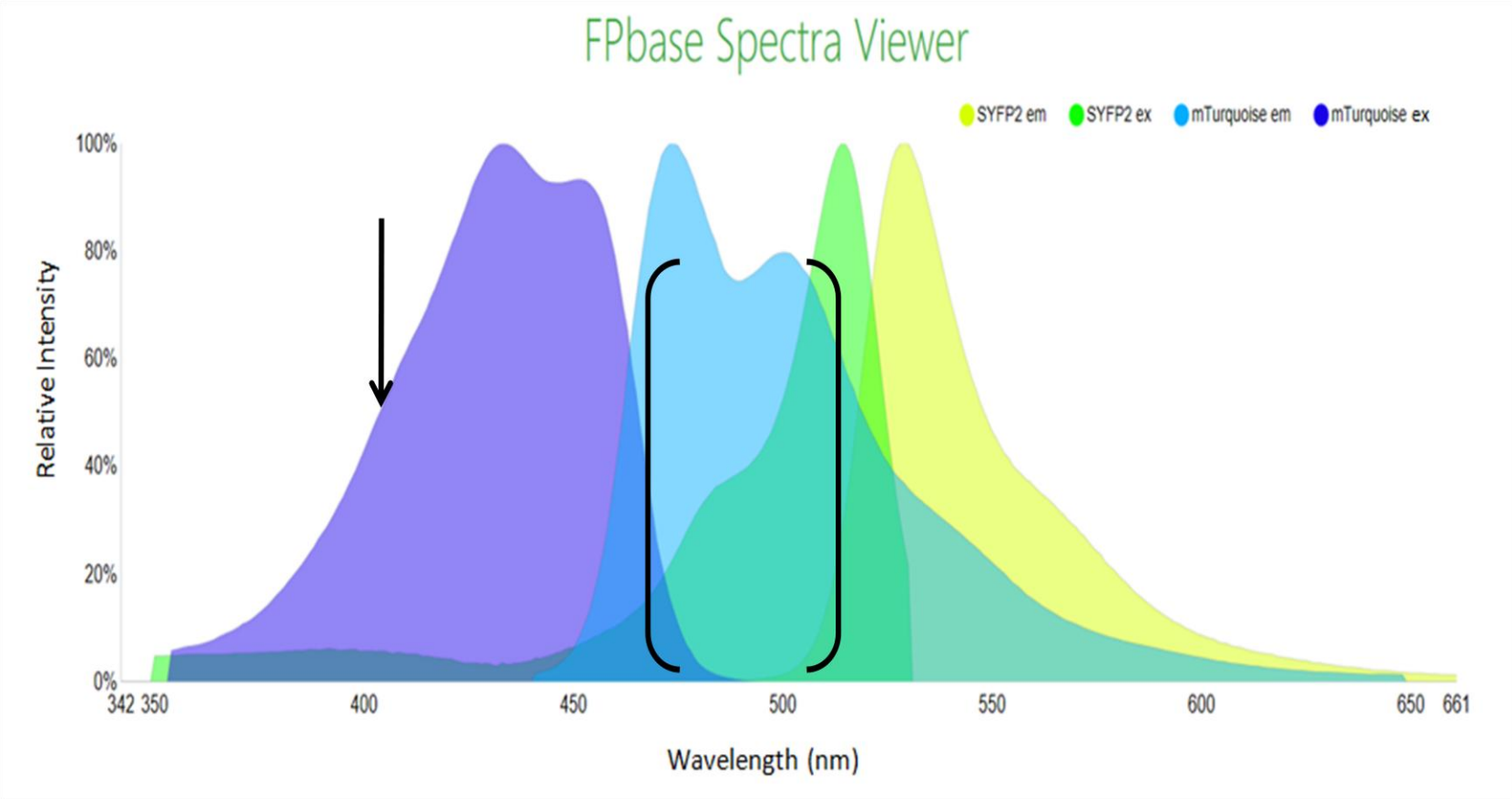

Figure 13: The spectral overlap between donor and acceptor fluorophores. There is a sizeable region of overlap between donor emission and acceptor excitation (seen in brackets) from which we obtain a FRET signal. There is virtually no overlap between the donor excitation (purple) and the acceptor emission (yellow). The peak excitation and emission of mTq are 434 and 474, respectively, and the peak excitation and emission of SYFP2 are 515 and 527 respectively. Arrow indicates 815 nm two-photon excitation used in the system which is equivalent to 407.5 nm for single-photon excitation. Image from FPbase.org

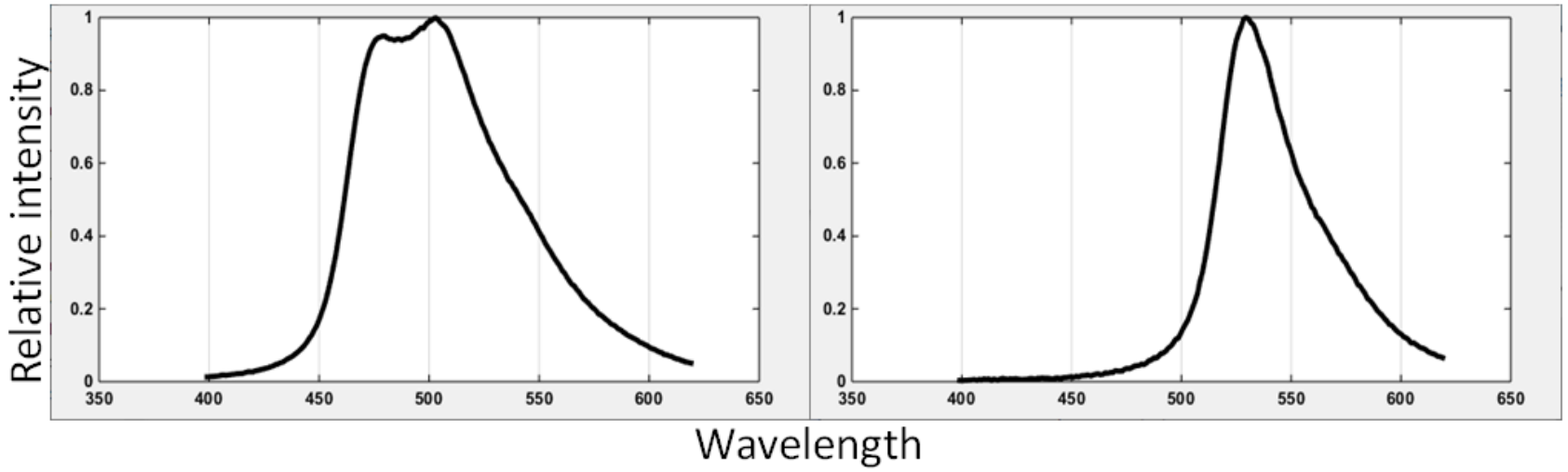

Figure 14: Representative elementary emission spectra constructed in the program OptiMiS_DC_2_7 from two photon excitation of donor (mTq, left) and acceptor (SYFP2, right) fluorophores from single transfectant cells for one set of experiments. The spectral integral values 88.12, and 54.25 for donor and acceptor, respectively, are used in determining FRET efficiency. A major advantage of using two-photon microscopy is the use of infrared wavelengths (815 nm for mTq, 930 nm for SYFP2) which are less harmful to living cells and tissues than lower, single photon excitation wavelengths.

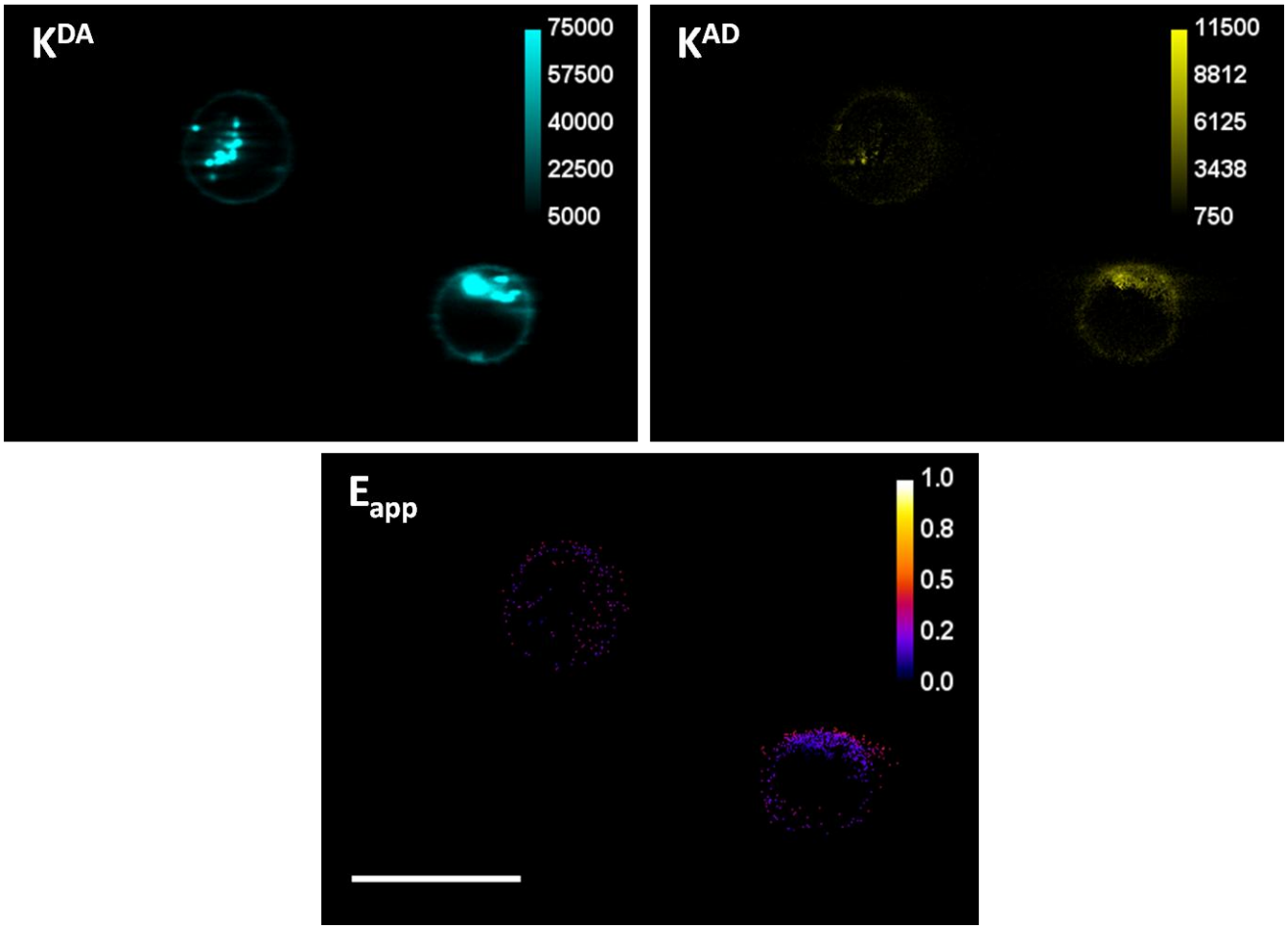

Figure 15: Representative FRET results from 815 nm excitation. Shown are K^{DA} which represents donor intensity in the presence of acceptor. In the pixels where FRET is occurring there is a decrease in fluorescence intensity of the donors because energy is being transferred to the acceptor. K^{AD} represents acceptor intensity in the presence of donor. Since we used 815 nm the acceptors are not excited therefore, what is shown in K^{AD} represents where energy is being transferred to acceptors. Scale bars in K^{AD} and K^{DA} fluorescence intensity. Both K^{DA} and K^{AD} are used to calculate apparent FRET efficiency. Lastly the E_{app} is shown, scale bar represents percent FRET efficiency. Most pixels here show less than 20% FRET efficiency. In general, few pixels present demonstrate FRET, which indicates a low degree of oligomerization and association of TF molecules. White scale bar in E_{app} image represents 10 µm.

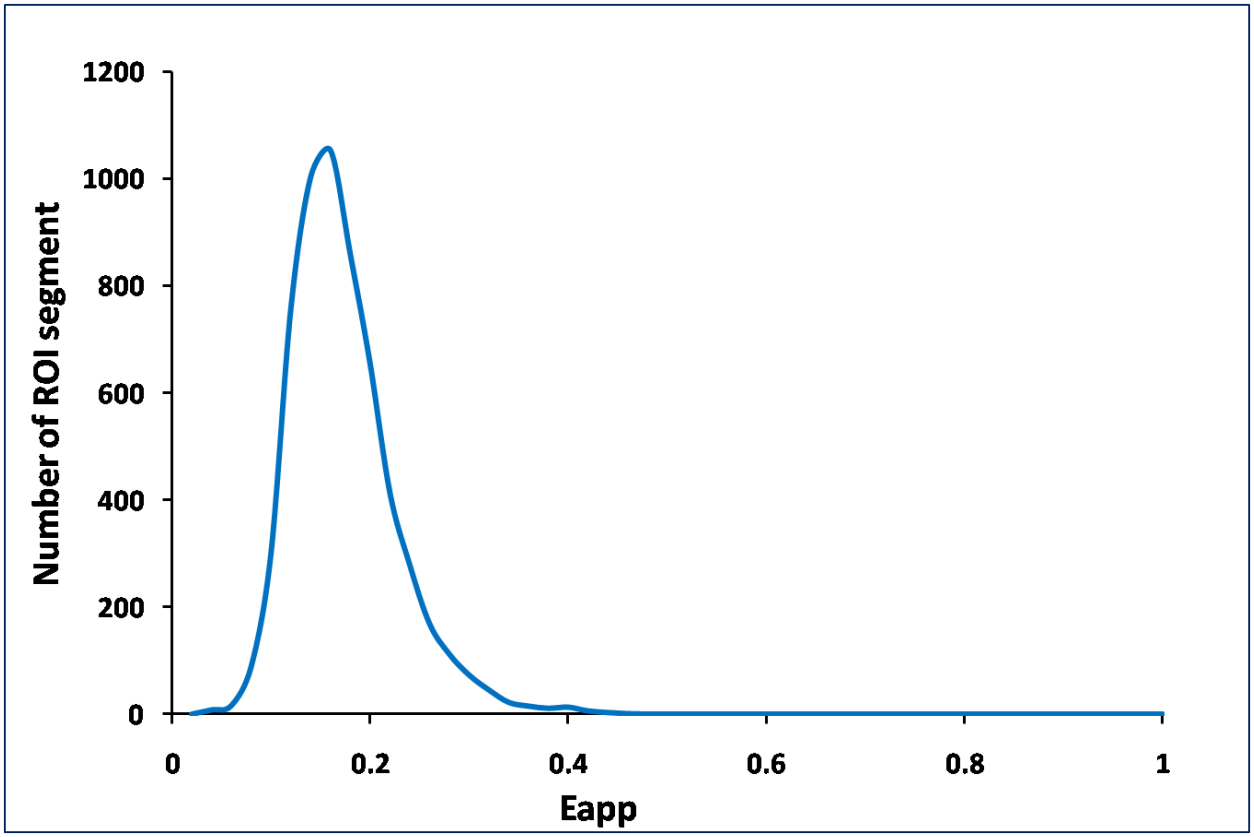

Figure 16: Meta histogram distribution of Eapp over 886 cells and 11566 ROI indicate TF exists as dimers. Modeling can predict the order of oligomerization based on the number of peaks present in meta histograms. Based on modeling the prominent narrow single peak signifies that TF on in 300.19 transfected cells are dimeric. Monomers are not detected in this analysis, therefore the proportion of total TF in dimers is unknown.

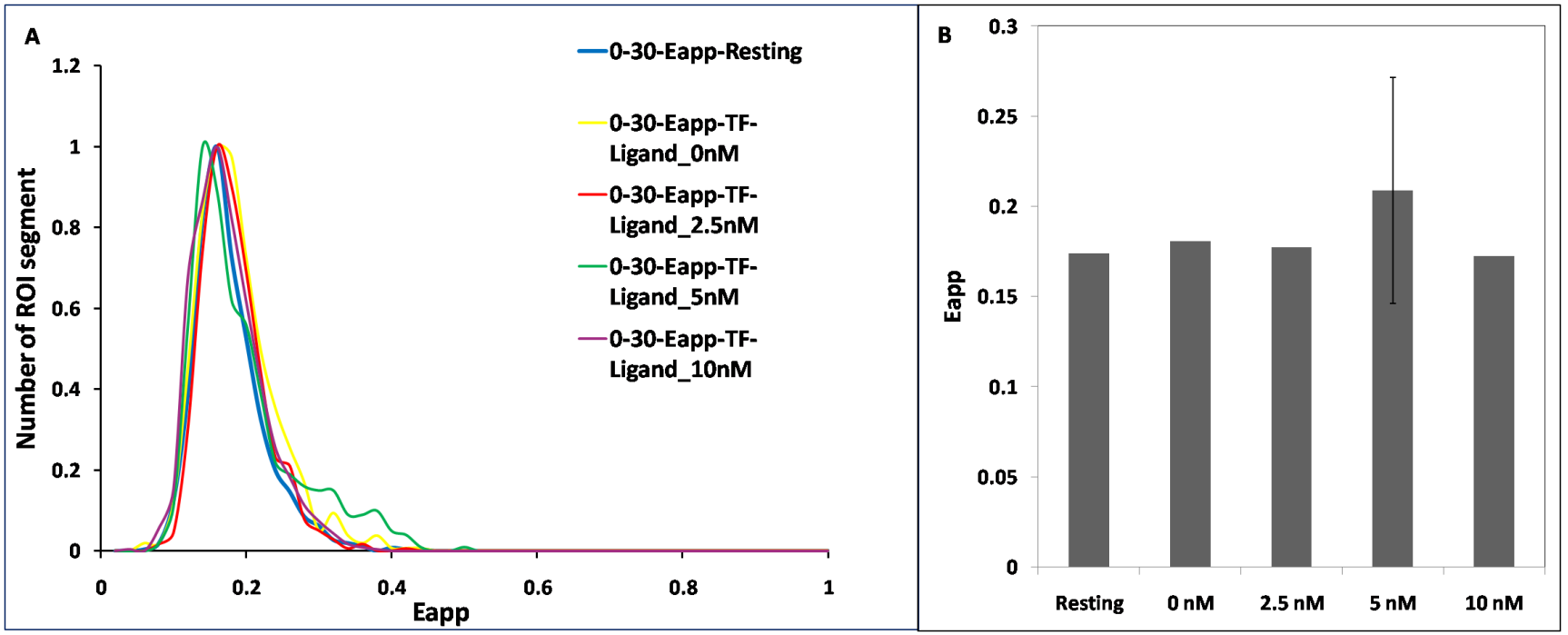

.

[F.VIIa]	Eapp Avg.	St. Dev.	# ROI	# Cells	# Experiments
Resting	0.174		1901	160	1
0 nM	0.181		1791	165	1
2.5 nM	0.177		1588	153	1
5 nM	0.209	0.063	2009	156	4
10 nM	0.172		1791	155	1

Figure 17: E_{app} at varying concentrations of F.VIIa reveals that addition of ligand has no effect of oligomeric structure of TF. A. Meta-histograms of E_{app} distributions. Regions of interest were selected for a concentration of 0-30 molecules/pixel. The single prominent peak seen at all concentrations of ligand tested means TF molecules associate as dimers regardless of the presence of F.VIIa. B. E_{app} values for specific concentrations of F.VIIa. Compared to the unperturbed cells, all concentrations of ligand tested show no significant difference in E_{app}, $p = 0.95$ according to ANOVA.

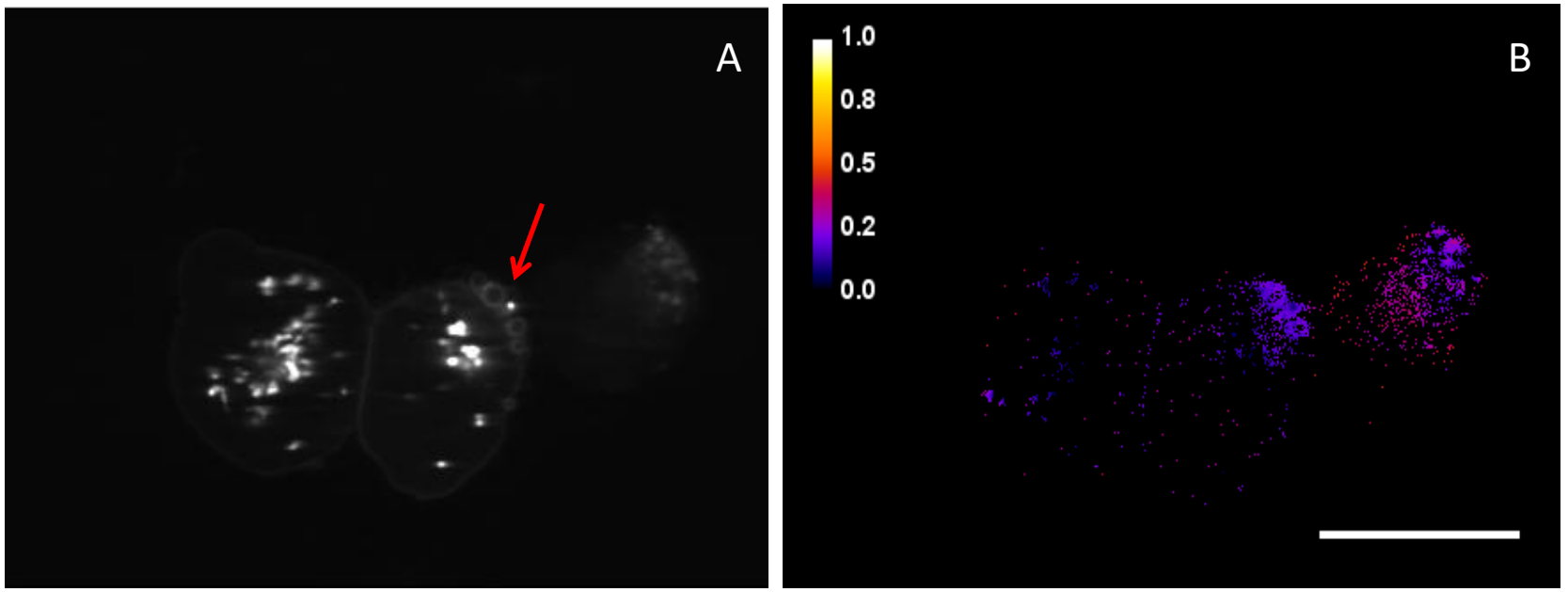

Figure 18: Microvesicles shed from cells stimulated with PMA have increased average FRET efficiency per region of interest. A. Donor only image of cell shedding microvesicles as indicated by the arrow. B. E_{app} map of image in A. The microvesicles have the same percent FRET efficiency as the whole cell from which they were presumably shed $p > 0.05$, nonetheless the average E_{app} per regions of interest is greater in regions of microvesicles than the membrane of the parent cell $p = 0.001$. p values based on results from t test. Scale bar represents 10 µm.

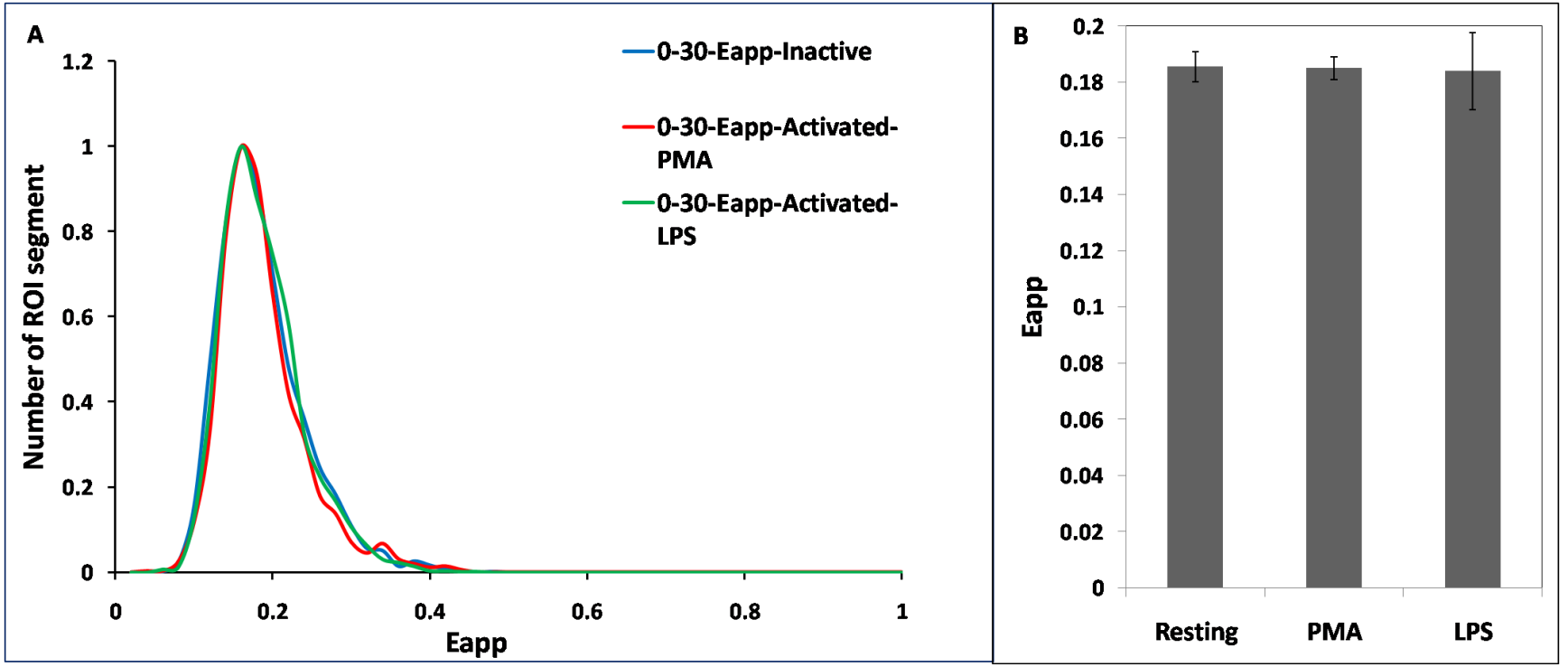

Stimulus	Eapp Avg.	St. Dev.	# ROI	# Cells	# Experiments
Resting	0.185	0.005	5153	405	4
PMA	0.185	0.004	4100	301	4
LPS	0.184	0.014	5281	393	4

Figure 19: Results with different treatments of activating agents reveals no significant change in E_{app}. A. Meta-histogram results show no significant shift in peak position between resting, PMA-, and LPS-activated cells, therefore no increase or decrease in FRET efficiency. This also suggests that there is no change in quaternary structure upon cell activation. If our hypothesis were correct we would expect to see a left shift in peak position indicating reduced FRET efficiency. 0-30 represents molecules/pixel. B. Average FRET results of 4 experiments from applying activating agents compared to resting 10.3 cells. The results show no significant change in E_{app} upon stimulus with PMA or LPS. p= 0.97 according to ANOVA.

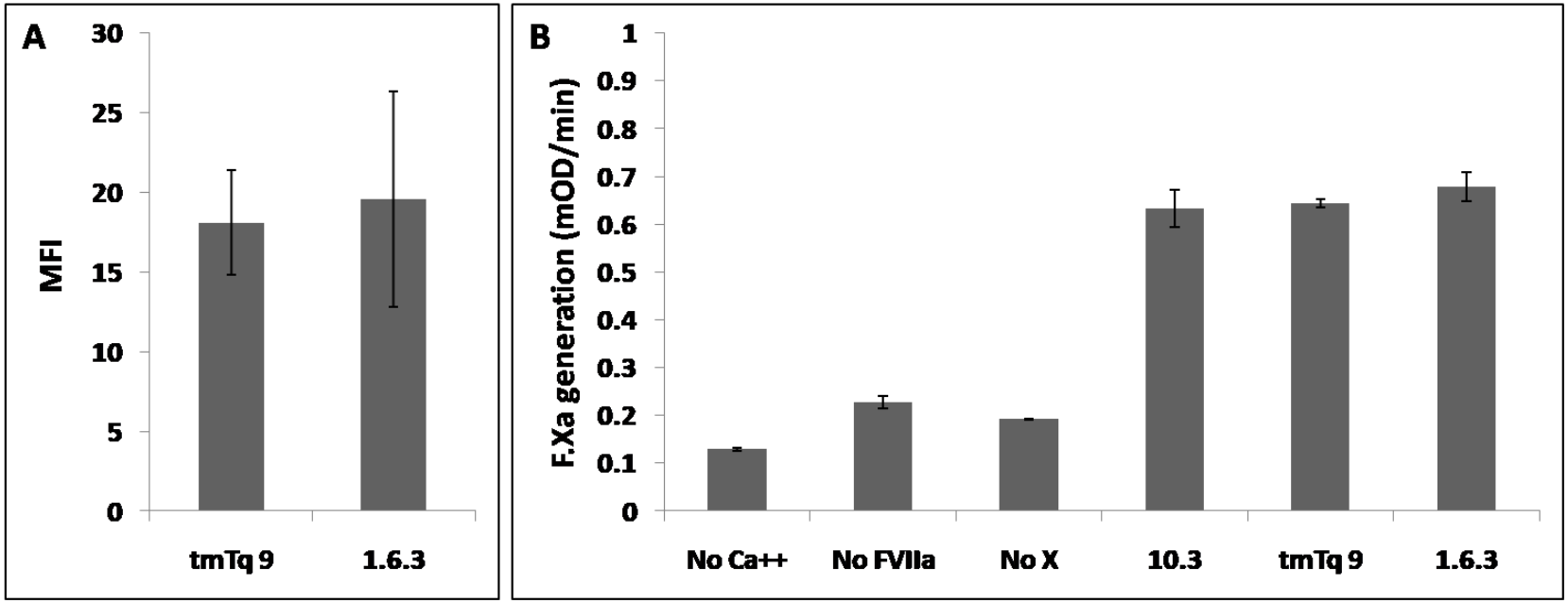

Figure 20: Fluorophore tagging of TF does not affect its procoagulant activity. A. MFI values of two cell lines used in activity assays: tmTq 9 represents the line with a fluorophore attached to the TF C-terminus and 1.6.3 represents the line without the fluorophore tag. Both lines have approximately equal levels of expression when labeled with an anti-TF monoclonal antibody and an Alexa Fluor 647-conjugated secondary antibody. Data obtained from three experiments, p= 0.76 according to two tailed t test, error bars represent standard deviation. B. F.Xa generation of three individual cell lines and controls using F.VIIa at a concentration of 0.2nM. No significant differences in F.Xa generation were observed between any of the cell lines tested. p = 0.77 according to ANOVA. Experiments were conducted three times with two replicates for each sample. Error bars represent standard deviation.

V: Discussion

A. Transfection and Subcloning

The 300.19 cell line model proved to be a very useful model for these studies. It is theoretically possible for endogenous murine TF to oligomerize with transfected human TF because TF is highly conserved. Oligomerization of endogenous TF with tagged, transfected TF would have decreased our ability to detect FRET. Our studies showed only low levels of FRET (~20% efficiency) in most ROI examined. A model system in which endogenous TF was available to associate with the tagged molecules may have eliminated our ability to detect oligomerization entirely.

Transfection generally leads to a heterogeneous population of cells. This is due to the number of copies of a plasmid that becomes integrated into the genome, the specific integration sites, and whether genome rearrangements occur.[75] We successfully created some homogenous cell lines that were used in FRET studies. The high sensitivity of FRET was desirable in order for us to easily detect a change in signal upon cell activation and/or ligand interaction. These homogenous lines also proved useful in comparing external expression levels for activity assays. While high variation in expression makes matching levels between lines a challenging task, we were able to isolate two equally expressing cell lines to compare in F.Xa generation studies.

Cell lines are used in vitro to model in vivo events. However, in vitro and in vivo are two very different systems. Regulatory mechanisms could greatly differ between primary cells in vivo and immortalized cell lines in vitro. In the literature, it has been noted that TF procoagulant

activity varies widely from cell type to cell type. This may be due in part to varying environments within the different cell surface membranes, and in part due to regulatory mechanisms specific to particular cell types. It is also noted that cells that naturally express TF could have regulatory components that are missing in TF transfected cells.[76]

B. FRET

The technique of FRET has been invaluable in our investigation. We have obtained FRET signal from resting cells, however it was only detected in small amounts. This is in agreement with the results by Bach and Moldow that less than half of TF molecules form oligomers.[64] Oligomerization is dependent on the concentration of the molecules present.[77] It is a possibility that FRET signal is not detected in abundance because even our highest expressing cell lines have relatively low total TF expression, and therefore lower concentrations of donor and acceptor molecules to make biological interactions. For the analysis 30 molecules/pixel were used for determining E_{app} because this range reduces the stochastic FRET. Stochastic FRET can occur when molecules are highly concentrated and make random interactions. Almost all of the data points from experiments were used in these samples because the average molecules/pixel on the 10.3 line was 17.

Our results on the effect of F.VIIa binding suggest that ligand does not influence TF oligomerization or E_{app}. However, it is important to note that these results come from a very limited number of samples. Testing of significantly more samples will be required to draw strong conclusions. Some variablity was introduced by leaving cells in the 5 nM F.VIIa sample concentrated as compared to the other doses, potentially affecting cell viability. Further variability may have come from baseline binding of F.VIIa present in the serum-containing

medium. An experimental design in which all samples were washed in EDTA before ligand addition to remove trace amounts of F.VIIa may have produced different results. Bovine F.VIIa in the serum supplement is expected to bind to TF molecules with high affinity, making the total concentration of F.VIIa bound after addition of varying amounts of human F.VIIa unknown. We must also point out that these experiments were conducted with transfected TF as opposed to natural TF, and the glycosylation may differ and affect the binding sites, giving them a higher or lower affinity for binding coagulation factors.[58]

This work provided one example of how average FRET efficiency per ROI on microvesicles is higher than on the cell from which they were presumably shed. This result is interesting; there may be higher oligomerization on microvesicles than on the cells that shed them. It is know that cancerous tumors can shed TF positive microvesicles which can lead to formation of the extrinsic tenase complex and cause clotting complications.[78] It was noticed in a study by Donate et al. that the dimeric form of TF, as opposed to its monomeric form, leads to the autoactivation of F.VII.[65] Therefore, TF dimerization could actually promote coagulation by activating more F.VII to F.VIIa to initiate coagulation. Despite the results from the microvesicle data it is important to note that many more samples need to be tested before a firm conclusion can be made and this is worth further investigation.

We hypothesized that TF exists as oligomers on quiescent cells and upon cellular activation these oligomers dissociate and leave the protein fully active to initiate coagulation. We tested this hypothesis by activating dually transfected cells with the potent stimulus PMA and the milder LPS and comparing the E_{app} to that observed on resting cells. Neither activating agent produced a significant change in E_{app} as compared to untreated cells. This implies that

oligomerization is not responsible for keeping TF in a cryptic state. If the self-association hypothesis were correct, then activating agents that decrypt TF activity would significantly reduce E_{app}. We therefore refute our hypothesis and conclude that the self-association hypothesis may not be responsible for regulating TF procoagulant activity. The underlying mechanism for activating TF may instead be the allosteric disulfide bond hypothesis.

Even though evidence in this research leads us to reject the hypothesis that disruption of TF dimers results in decryption, we have still gained valuable insight. Oxidation of the Cys186-Cys209 allosteric disulfide bond may be important in TF oligomerization as well as playing a key role in the transformation of TF to its procoagulant form. Thus, the two mechanisms could potentially both contribute to development of full TF procoagulant activity. If a cell line with higher concentrations of the tagged TF molecules were available, it may allow us to detect a change in oligomerization through measuring FRET efficiency although, having higher levels of expression on these cells may not be physiologically relevant. If the mechanism of decryption was fully understood, this could be helpful for patients by leading to strategies to keep TF in a cryptic state to treat and prevent clotting complications.

C. Activity Assays

Interestingly, the 10.3 dually transfected cell line had much higher expression of TF molecules as compared to the two lines matched for levels of TF antigen present on the cell surface, yet displayed the same level of F.Xa-generating activity. This unexpected result may be because most TF molecules exist in the cryptic form and are unable to drive F.Xa production. Since this line expresses more copies of the TF molecule, this suggests that it has a higher proportion of molecules in the cryptic state than its lower-expressing counterparts. Previous

studies have shown that some cell lines exhibit lower amounts of F.Xa generation compared to other cell lines even though these lines express more molecules/cell and has approximately equal percentages of cryptic TF (refer to Table 1)[66]. Another reason why the 10.3 line may not have produced more F.Xa could be due to the F.VIIa concentration being the limiting factor because 0.2 nM was used as opposed to saturating amounts.

The activity assays confirmed there was no significant difference between an untagged protein and a fluorphore-tagged protein in their ability to support F.Xa generation. Given that the fluorophore in these constructs is attached to the cytoplasmic domain and the extracellular domain is responsible for binding F.VIIa and F.X, we did not expect a significant effect of the fluorophore on ligand binding. Likewise, we considered it unlikely that the fluorophore would affect the proteolytic activity of the TF-F.VIIa complex, and in fact, the reporter on the C-terminus of TF did not affect the procoagulant capacity of the molecule. Nevertheless, attachment of a reporter to the C-terminus may interfere with critical interactions of the molecule with its phospholipid environment or its intracellular signaling mechanisms. Because effective F.Xa generation depends on the exposure of phosphatidylserine, equivalent production suggests that the cytoplasmic fluorophore tag does not affect how TF interacts with the surrounding membrane. The potential effects of a cytoplasmic reporter on downstream signaling have not been addressed in this study. These results support the broad conclusion that the fluorophore-tagged proteins commonly used in a wide range of biological model systems have unaltered function and can be considered to be excellent models of the normal protein.

VI. Conclusion

To conclude this work, we have addressed the self-association hypothesis of TF regulation, whether ligand interactions affect TF oligomerization, and whether a fluorophore attached to the C-terminus of TF affects its function. First, we have found that the predominant form of TF oligomers on live, stably transfected 300.19 cells are dimers. This appears to be unchanged by cell activation with either potent stimulation by PMA or with mild stimulation by LPS, suggesting that self-association does not explain how TF is encrypted. We have also shown that the addition of ligand F.VIIa does not appear to affect oligomerization. After over 100 years of TF research, many mysteries remain, including the mechanism by which TF is activated to initiate coagulation. If we can unravel the mystery of TF decryption, treatments can be designed to turn decrypted TF back to the cryptic form or keep TF cryptic in disease states where the protein is aberrantly expressed or activated. Finally, the model system we have employed in these studies provides direct evidence that fusion of this protein with a fluorescent moiety does not impair its biological function.

In the future it would be desirable to screen additional tagged TF-expressing cell lines in order to isolate clones with higher levels of expression. These could be used to further investigate the proportion of TF oligomers as measured by E_{app} as compared to the results in this study, or whether cell activation with LPS or PMA alters the TF oligomeric structure. It would also be useful to analyze the microvesicles shed from activated cells by comparing average E_{app} and oligomerization over regions of interest from the microvesicles to whole cells from which they were shed. The unimpaired function of fluorescently tagged proteins could be further explored by investigating the function of TF constructs with the fluorophore attached to

the N-terminus of the molecule. Further analysis to investigate the effect of a C-terminal fluorophore tag on TF signaling by using immunohistochemistry to detect phosphorylation of the cytoplasmic tail would be of great interest. If phosphorylation has occurred then no measurable change had occurred, our conclusion that fluorophore tags do not affect the biological function of proteins could be applied very broadly.

References

1. Bachli E. History of tissue factor. *Br J Haematol*. 2000; 110(2):248-255.
2. Grover S.P., Mackman N. Tissue factor: an essential mediator of hemostasis and trigger of thrombosis. *Arterioscler Thromb Vasc Biol*. 2018;38(4):709-725.
3. Marowitz P. Die chemie der blutgerinnung. *Ergebnisse der Physiol*. 1905;4:307-422.
4. Davie E.W., Ratnoff O.D. Waterfall sequence for intrinsic blood clotting. *Science*. 1964;145(3638):1310-1312.
5. Macfarlane R. An enzyme cascade in the blood clotting mechanism, and its function as a biochemical amplifier. *Nature*. 1964;202:498-499.
6. Osterud B., Rapaport S.I. Activation of factor IX by the reaction product of tissue factor and factor VII: additional pathway for initiating blood coagulation. *Proc Natl Acad Sci U S A*. 1977;74(12):5260-5264.
7. Douglas S. Coagulation history, Oxford 1951-53. *Br J Haematol*. 1999;107:22-32.
8. Scarpati E.M., Wen D., Broze G.J., Milethich J.P., Flandermeyer R.R, Siegel N.R, Sadler J.E, Human tissue factor: cDNA sequence and chromosome localization of the gene. *Biochemistry*. 1987;26(17):5234-5238.
9. Fisher K.L., Gorman C.M., Vehar G.A., O'Brien D.P., Lawn R.M. Cloning and expression of human tissue factor cDNa. *Thromb Res*. 1987;48(1):89-99.
10. Morrissey J.H, Fakhrai H., Edgington T.S. Molecular cloning of the cDNA for tissue factor, the cellular receptor for the initiation of the coagulation protease cascade. *Cell*. 1987;50(1):129-135.
11. Spicer E.K, Horton R., Bloem L., et al. Isolation of cDNA clones coding for human tissue factor: primary structure of the protein and cDNA. *Proc Natl Acad Sci U S A*. 1987;84(15):5148-5152.
12. Butenas S. Tissue factor structure and function. *Scientifica*. 2012;2012:1-15.
13. Palta S., Saroa R., Palta A. Overview of the coagulation system. *Indian J Anaesth*. 2014;58(4):515-523
14. Hoffman M., Monroe D.M., Oliver J.A., Roberts H.R. Factors IXa and Xa play distinct roles in tissue factor-dependent initiation of coagulation. *Blood*. 1995;86(5):1794-1801
15. Smith S.A., Travers R.J., Morrissey J.H. Initiation of clotting cascade. *Crit Rev Biochem Mol Biol*. 2016;50(4):326-336.
16. Norledge B.V, Petrovan R.J., Wolfram R., Olsen A.J. The tissue factor/factor VIIa/factor Xa complex: a model built by docking and site-directed mutagenesis. *Proteins Struct Funct Genet*. 2003;53(3):640-648.
17. Wiggins R.C., Bouma B.N., Cochrane C.G., Griffin J.H. Role of high-molecular-weight kininogen in surface-binding and activation of coagulation factor XI and prekallikrein. *Proc Natl Acad Sci U S A*. 1977;74(10):4636-4640.
18. Grover S.P., Mackman N. Intrinsic pathway of coagulation and thrombosis: insights from animal models. *Arterioscler Thromb Vasc Biol*. 2019;39(3):331-338.
19. Oliver J.A., Monroe D.M., Roberts H.R., Hoffman M. Thrombin activates factor XI on activated platelets in the absence of factor XII. *Arterioscler Thromb Vasc Biol*. 1999;19(1):170-177.
20. Sevinsky J.R., Rao L.V., Ruf W. Ligand-induced protease receptor translocation into caveolae: a mechanism for regulating cell surface proteolysis of the tissue factor-

dependent coagulation pathway. *J Cell Biol*. 1996;133(2):293-304.
21. Rao L.V.M., Kothari H., Pendurthi U.R. Tissue factor: mechanisms of decryption. *Front Biosci - Elit*. 2012;4 E(4):1513-1527.
22. Toomey J.R., Kratzer K.E., Lasky N.M., Stanton J.J., Broze G.J. Targeted disruption of the murine tissue factor gene results in embryonic lethality. *Blood*. 1996;88(5):1583-1587.
23. Bugge T.H., Xiao Q., Kombrinck K.W., et al. Fatal embryonic bleeding events in mice lacking tissue factor , the cell-associated initiator of blood coagulation. 1996;93(June):6258-6263.
24. Carmeliet P., Mackmant N., Moons L., et al. Role of tissue factor in development. 1996;383:73-75.
25. Mackman N. Role of tissue factor in hemostasis, thrombosis, and vascular development. *Arterioscler Thromb Vasc Biol*. 2004;24(6):1015-1022.
26. Chen J., Kasper M., Heck T., et al. Tissue factor as a link between wounding and tissue repair. *Diabetes*. 2005;54(7):2143-2154.
27. Drake T.A., Morissey J.H., Edgington T.S. Selective cellular expression of tissue factor in human tissues. Implications for disorders of hemostasis and thrombosis. *Am J Pathol*. 1989;134(5):1087-1097.
28. Eddleston M., De La Torre J.C., Oldstone M.B.A., Loskutoff D.J., Edgington T.S., Mackman N. Astrocytes are the primary source of tissue factor in the murine central nervous system: a role for astrocytes in cerebral hemostasis. *J Clin Invest*. 1993;92(1):349-358.
29. Bode M., Mackman N. Regulation of tissue factor gene expression in monocytes and endothelial cells: thromboxane A2 as a new player. *Vasc Pharmacol*. 2015;62(2):57-62.
30. Rothmeier A.S., Marchese P., Langer F., et al. Tissue factor prothrombotic activity is regulated by integrin-arf6 trafficking. *Arterioscler Thromb Vasc Biol*. 2017;37(7):1323-1331.
31. Langer F., Ruf W. Synergies of phosphatidylserine and protein disulfide isomerase in tissue factor activation. *Thromb Haemost*. 2014;111(4)590-597
32. Toschi V., Gallo R., Lettino M., et al. Tissue factor modulates the thrombogenicity of human atherosclerotic plaques. *Circulation*. 1997;95(3):594-599.
33. Hidesakua A., Yukiob S., Tomotakac Y., et al. Pathophysiology of disseminated intravascular coagulation (DIC) progresses at a different rate in tissue factor-induced and lipopolysaccharide-induced DIC models in rats. *Blood Coagul Fibrinolysis*. 2003;14(3):221-228.
34. Khorana A.A., Ahrendt S.A., Ryan C.K., et al. Tissue factor expression, angiogenesis, and thrombosis in pancreatic cancer. *Clin Cancer Res*. 2007;13(10):2870-2875.
35. Yu J.L., May L., Lhotak V., et al. Oncogenic events regulate tissue factor expression in colorectal cancer cells: Implications for tumor progression and angiogenesis. *Blood*. 2005;105(4):1734-1741.
36. Hisada Y., Mackman N. Tissue factor and cancer: regulation, tumor growth, and metastasis. *Semin Thromb Hemost*. 2019;45(4):385-395.
37. Thaler J., Ay C., Mackman N. et al. Microparticle-associated tissue factor activity, venous thromboembolism and mortality in pancreatic, gastric, colorectal and brain cancer patients. *J Thromb Haemost*. 2012;10(7):1363-1370.
38. Van Den Berg Y.W., Osanto S., Reitsma P.H., Versteeg H.H. The relationship between

tissue factor and cancer progression: Insights from bench and bedside. *Blood*. 2012;119(4):924-932.
39. Déry O., Corvera C.U., Steinhoff M.,Bunnet N.W. Proteinase-activated receptors: novel mechanisms of signaling by serine proteases. *Am J Physiol*. 1998;274(6):C1429-C1452.
40. Vu T.K., Wheaton W.I., Hung D.T., Charo I., Coughlin S.R. Domains specifying thrombin-receptor interaction. *Nature*. 1991;353:674-677.
41. Ahamed J., Ruf W. Protease-activated receptor 2-dependent phosphorylation of the tissue factor cytoplasmic domain. *J Biol Chem*. 2004;279(22):23038-23044.
42. Carson S.D., Henry W.M., Shows T.B. Tissue factor gene localized to human chromosome 1 (1pter----1p21). *Science*. 1985;229(4717):991-993.
43. Boltzena U., Eisenreicha A., Antoniak S., et al. Alternatively spliced tissue factor and full-length tissue factor protect cardiomyocytes against TNF-α-induced apoptosis. *J Mol Cell Cardiol*. 2012;52(5):1056–1065.
44. Bazan J.F. Structural design and molecular evolution of a cytokine receptor superfamily. *Proc Natl Acad Sci U S A*. 1990;87(18):6934-6938.
45. Gorby C., Martinez-Fabregas J., Wilmes S., Moraga I. Mapping determinants of cytokine signaling via protein engineering. *Front Immunol*. 2018;9:2143.
46. Versteeg H.H., Ruf W. Emerging insights in tissue factor-dependent signaling events. *Semin Thromb Hemost*. 2006;32(1):24-32.
47. Maikel P., Henri V. In silico tissue factor analysis : a bit-to-bit comparison *Thromb Haemost*. 2003;89:592-593.
48. Zhou B., Hogg P.J., Gräter F. One-way allosteric communication between the two disulfide bonds in tissue factor. *Biophys J*. 2017;112(1):78-86.
49. Bach R.R. Tissue factor encryption. *Arterioscler Thromb Vasc Biol*. 2006;26(3):456-461.
50. Rao L.V.M., Pendurthi U.R. Regulation of tissue factor coagulant activity on cell surfaces. *J Thromb Haemost*. 2012;10(11):2242-2253
51. Dzung T.L, Rapaport S.I., Rao L.V.M. Relations between factor VIIa binding and expression of factor VIIa/tissue factor catalytic activity on cell surfaces. *J Biol Chem*. 1992;267(22):15447-15454.
52. Chen V.M., Hogg P.J. Encryption and decryption of tissue factor. *J Thromb Haemost*. 2013;11 Suppl 1:277-284.
53. Chen V.M., Ahamed J., Versteeg H.H., Berndt M.C., Ruf W., Hogg P.J. Evidence for activation of tissue factor by an allosteric disulfide bond. *Biochemistry*. 2006;45(39):12020-12028.
54. Sezgin E., Levental I., Mayor S., Eggeling C. The mystery of membrane organization: composition, regulation and physiological relevance of lipid rafts. *Nat Rev Mol Cell Biol*. 2017;18(6):361-374.
55. Dietzen D.J., Page K.L., Tetzloff T.A. Lipid rafts are necessary for tonic inhibition of cellular tissue factor procoagulant activity. *Hemostasis, Thromb Vasc Biol*. 2004;103(8):3038-3044.
56. Mandal S.K., Iakhiaev A., Pendurthi U.R., Rao L.V.M. Acute cholesterol depletion impairs functional expression of tissue factor in fibroblasts : modulation of tissue factor activity by membrane cholesterol. *Hemostasis, Thromb Vasc Biol*. 2005;105(1):153-160.
57. Ohtsubo K., Marth J.D. Glycosylation in cellular mechanisms of health and disease. *Cell*.

2006;126(5):855-867.
58. Krudysz-Amblo J., Jennings M.E., Mann K.G., Butenas S. Carbohydrates and activity of natural and recombinant tissue factor. *J Biol Chem*. 2010;285(5):3371-3382.
59. Rehemtulla A., Ruf W., Edgington T.S. The integrity of the cysteine 186-cysteine 209 bond of the second disulfide loop of tissue factor is required for binding of factor VII. *J Biol Chem*. 1991;266(16):10294-10299.
60. Kothari H., Rao L.V.M., Pendurthi U.R. Glycosylation of tissue factor is not essential for its transport or functions. *J Thromb Haemost*. 2011;9(8):1511-1520.
61. Versteeg H.H., Ruf W. Tissue factor coagulant function is enhanced by protein-disulfide isomerase independent of oxidoreductase activity. *J Biol Chem*. 2007;282(35):25416-25424.
62. Bach R.R., Monroe D. What is wrong with the allosteric disulfide bond hypothesis? *Arterioscler Thromb Vasc Biol*. 2009; 29(12):1997-1998
63. Ruf W. Role of thiol pathways in TF procoagulant regulation. *Thromb Res*. 2012;129:S11-S12.
64. Bach R.R, Moldow C.F. Mechanism of tissue factor activation on HL-60 cells. *Blood*. 1997;89(9)3270-3276
65. Don F., Kelly C.R., Ruf W., Edgington T.S. Dimerization of tissue factor supports solution-phase autoactivation of factor VII without Influencing proteolytic activation of factor X. *Biochemistry*. 2000;39:11467-11476.
66. Kothari H., Pendurthi U.R., Roa L.V.M. Analysis of tissue factor expression in various cell model systems: cryptic vs. active. *J Thromb Haemost*. 2014;11(7):1353-1363.
67. Gragg M., Park P.S.H. Detection of misfolded rhodopsin aggregates in cells by förster resonance energy transfer. *Methods Cell Biol.* 2019;149:87-105
68. Alt F., Rosenberg N., Lewis S., Thomas E., Baltimore D. Organization and reorganization of immunoglobulin genes in A-MuLV-transformed cells: rearrangement of heavy but not light chain genes. *Cell*. 1981;27:381-390.
69. Singh D.R., Mohammad M.M, Patowarya S., Stoneman M.R., Oliver J.A., Movileanud L., Raicu V. Determination of the quaternary structure of a bacterial ATPbinding cassette (ABC) transporter in living cells. *Integr Biol*. 2013;5(2):312–323.
70. Patowary S., Alvarez-Curto E., Xu T.R., Holz J.D., Oliver J.A., Milligan G., Raicu V. The muscarinic M3 acetylcholine receptor exists as two differently sized complexes at the plasma membrane. *Biochem J*. 2013;452(2):303-312.
71. Raicu V., Singh D.R. FRET spectrometry: a new tool for the determination of protein quaternary structure in living cells. *Biophys J*. 2013;105(9):1937-1945.
72. Wallace B., Atzberger P.J. Forster resonance energy transfer: role of diffusion of fluorophore orientation and separation in observed shifts of FRET efficiency. *PLoS One*. 2017;12(5):1-22
73. Raicu V., Stoneman M.R., Fung R., et al. Determination of supramolecular structure and spatial distribution of protein complexes in living cells. *Nat Photonics*. 2009;3(2):107-113.
74. The fluorecent protein database. https://www.fpbase.org.
75. Vogl T., Gebbie L., Palfreyman R.W., Speight R. Effect of plasmid design and type of integration event on recombinant protein expression in *Pichia pastoris*. *Appl Environ Microbiol*. 2018;84(6):1-16

76. Wolberg A.S., Kon R.H., Monroe D.M., Ezban M., Roberts H.R., Hoffman M. Deencryption of cellular tissue factor is independent of its cytoplasmic domain. *Biochem Biophys Res Commun*. 2000;272(2):332-336.
77. Mishra A.K., Gragg M., Stoneman M.R., et al. Quaternary structures of opsin in live cells revealed by FRET spectrometry. *Biochem J*. 2016;473(21)3819-3836.
78. Ender F., Freund A., Quecke T., Steidel C., Zamzow P., Von Bubnoff N., Gieseler F. Tissue factor activity on microvesicles from cancer patients. *J Cancer Res Clin Oncol*. 2020;146(2):467-475.